# Validation of Aura Microwave Limb Sounder stratospheric ozone measurements

L. Froidevaux,[1] Y. B. Jiang,[1] A. Lambert,[1] N. J. Livesey,[1] W. G. Read,[1] J. W. Waters,[1] E. V. Browell,[2] J. W. Hair,[2] M. A. Avery,[2] T. J. McGee,[3] L. W. Twigg,[4] G. K. Sumnicht,[4] K. W. Jucks,[5] J. J. Margitan,[1] B. Sen,[1] R. A. Stachnik,[1] G. C. Toon,[1] P. F. Bernath,[6,7] C. D. Boone,[7] K. A. Walker,[7,8] M. J. Filipiak,[9] R. S. Harwood,[9] R. A. Fuller,[1] G. L. Manney,[1,10] M. J. Schwartz,[1] W. H. Daffer,[1] B. J. Drouin,[1] R. E. Cofield,[1] D. T. Cuddy,[1] R. F. Jarnot,[1] B. W. Knosp,[1] V. S. Perun,[1] W. V. Snyder,[1] P. C. Stek,[1] R. P. Thurstans,[1] and P. A. Wagner[1]

Received 10 April 2007; revised 14 November 2007; accepted 11 January 2008; published 9 May 2008.

[1] The Earth Observing System (EOS) Microwave Limb Sounder (MLS) aboard the Aura satellite has provided essentially daily global measurements of ozone ($O_3$) profiles from the upper troposphere to the upper mesosphere since August of 2004. This paper focuses on validation of the MLS stratospheric standard ozone product and its uncertainties, as obtained from the 240 GHz radiometer measurements, with a few results concerning mesospheric ozone. We compare average differences and scatter from matched MLS version 2.2 profiles and coincident ozone profiles from other satellite instruments, as well as from aircraft lidar measurements taken during Aura Validation Experiment (AVE) campaigns. Ozone comparisons are also made between MLS and balloon-borne remote and in situ sensors. We provide a detailed characterization of random and systematic uncertainties for MLS ozone. We typically find better agreement in the comparisons using MLS version 2.2 ozone than the version 1.5 data. The agreement and the MLS uncertainty estimates in the stratosphere are often of the order of 5%, with values closer to 10% (and occasionally 20%) at the lowest stratospheric altitudes, where small positive MLS biases can be found. There is very good agreement in the latitudinal distributions obtained from MLS and from coincident profiles from other satellite instruments, as well as from aircraft lidar data along the MLS track.

**Citation:** Froidevaux, L., et al. (2008), Validation of Aura Microwave Limb Sounder stratospheric ozone measurements, *J. Geophys. Res.*, *113*, D15S20, doi:10.1029/2007JD008771.

## 1. Introduction

[2] High-quality ozone measurements in the current declining phase of stratospheric chlorine [e.g., *Froidevaux et al.*, 2006b] are essential to better understand the expected beginning of a slow recovery phase for this important stratospheric gas. Ground-based and satellite measurements of ozone columns provide the requisite time series for assessing expected changes in solar ultraviolet (UV) flux at the ground. Global ozone profile measurements should enable a more thorough understanding of atmospheric forcing and response, including constraints on atmospheric models and their predictive capabilities. Recently, there has been a break in the global long-term series of high-quality ozone profile data from the Stratospheric Aerosol and Gas Experiment (SAGE) series of occultation measurements, covering the period 1979 to 2005, from the Upper Atmosphere Research Satellite (UARS) Halogen Occultation Experiment (HALOE) measurements (1991 to 2005), and from the Polar Ozone and Aerosol Measurement (POAM) experiments (1993 to 2005). The Canadian Space Agency's SCISAT mission [*Bernath et al.*, 2005], launched in August 2003 is helping to continue this series of solar occultation measurements. The 15 July 2004 launch of the Aura satellite, with four remote sensors on board [*Schoeberl et al.*, 2006a], has led to a new and extensive data set about the Earth's atmospheric composition. This includes continuous,

[1]Jet Propulsion Laboratory, California Institute of Technology, Pasadena, California, USA.
[2]NASA Langley Research Center, Hampton, Virginia, USA.
[3]NASA Goddard Space Flight Center, Greenbelt, Maryland, USA.
[4]Science Systems Applications, Inc., Lanham, Maryland, USA.
[5]Harvard-Smithsonian Center for Astrophysics, Cambridge, Massachusetts, USA.
[6]University of York, York, UK.
[7]University of Waterloo, Waterloo, Ontario, Canada.
[8]University of Toronto, Toronto, Ontario, Canada.
[9]University of Edinburgh, Edinburgh, UK.
[10]Also at New Mexico Institute of Mining and Technology, Socorro, New Mexico, USA.

Copyright 2008 by the American Geophysical Union.
0148-0227/08/2007JD008771

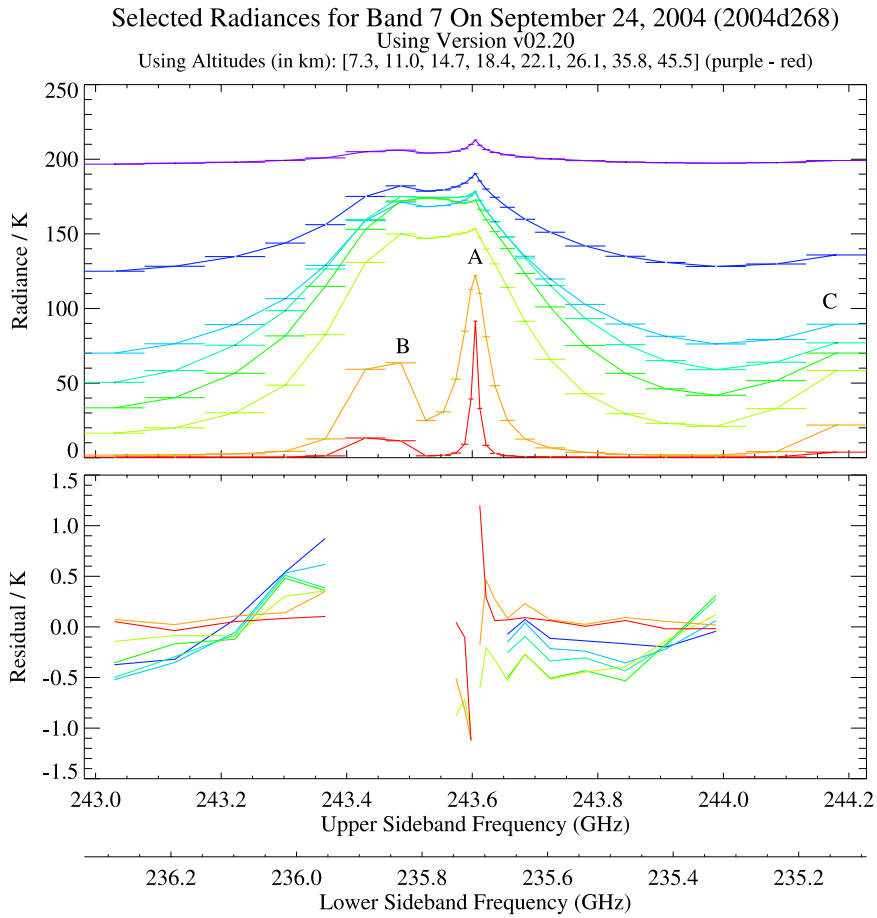


**Figure 1.** (top) MLS daily average radiances for the "band 7" spectral region near 240 GHz, relevant to the retrievals of the MLS standard $O_3$ product. The width of the channel filters is indicated by horizontal lines. The primary ozone emission line occurs in the lower sideband and is seen near the center of the plot (label A), with weaker ozone lines (from the upper sideband, folded over in this plot) to the left of it (label B), and wing emission from another line to the right (label C). These radiances are for 24 September 2004 for average tangent heights of 7 km (purple) to 45 km (red), as indicated above the plot. The x axes provide the frequencies in the upper and lower sidebands, which both contribute to the total radiances measured by MLS. (bottom) Residuals (average calculated minus observed radiances) corresponding to each colored curve from Figure 1 (top). Channels that are not shown here are not used in the retrievals, except for the very center of the main line, which is covered by fine-resolution digital autocorrelator spectrometer (DACS) channels for the mesosphere. Also, optical depth cut-off criteria "turn off" certain channels (near-line center) at the lower altitude levels.

day and night global measurements by the Earth Observing System (EOS) Microwave Limb Sounder (MLS) instrument, which detects thermal emission from trace gases at millimeter to submillimeter wavelengths [*Waters et al.*, 2006]; EOS MLS will mostly be referred to here as MLS, or Aura MLS.

[3] In this paper, we present validation results for MLS stratospheric ozone, with some comments on the upper (mesospheric) range of these data. Although MLS measures ozone ($O_3$) in several spectral bands, this paper focuses on the "standard product," retrieved from radiance measurements near 240 GHz (MLS radiometer 3, or "R3"), and providing the best precision for the widest vertical range. Version 2.2 (or v2.2), the 2nd public release of MLS data, started its "forward processing" mode in March 2007, and is currently in the reprocessing stages, with a more limited set of days available than v1.5; close to 300 d (10 months) of version 2.2 data were available at time of writing, with an emphasis on special months or days of interest for validation, primarily between September 2004 and July 2006. Comparisons discussed here that do not use MLS data past the end of 2005 have less than 160 d of reprocessed MLS data available. A few months did not have any reprocessed days, namely December 2004 and April, May, July, and August 2005. The results shown here are quite representative nevertheless. The MLS v2.2 data are the validation focus of this paper, since this data version is the more definitive and improved version. A subsequent data version, labeled 2.21, includes a minor software patch that affects the treatment of bad Level 1 radiances, but with essentially no impact on days that have been reprocessed; the available v2.20 data can therefore be safely used, and we refer to

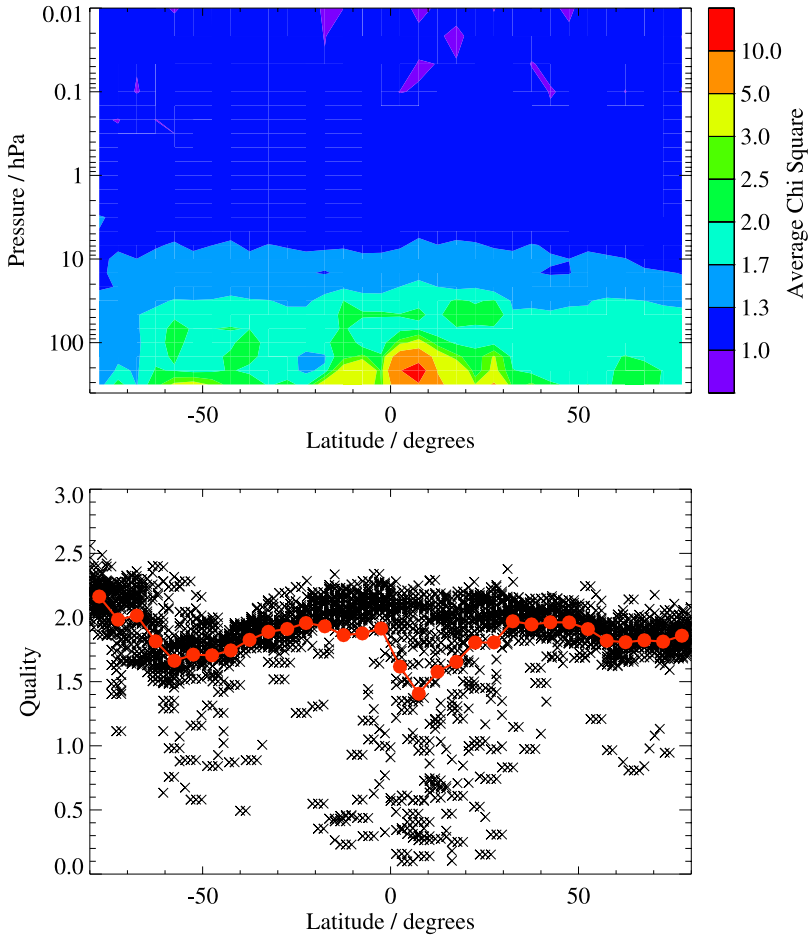


**Figure 2.** (top) Zonal mean chi square values (see text) representing the goodness of radiance fits versus latitude and pressure for the main MLS ozone band (band 7) on 24 September 2004. (bottom) Values of the related ozone Quality field, which is a single number measure of the radiance fits for each profile. Crosses give each Quality value versus latitude, and the red dots represent zonal mean Quality values.

these and other days using v2.21 collectively as v2.2. The stratospheric $O_3$ changes between the two versions are quite systematic in nature, and typically of order 10% or less. Our earlier analyses using v1.5 [*Froidevaux et al.*, 2006a] demonstrated generally good comparisons (often within 5–10%) versus correlative data for January through March 2005. Some perspective with respect to the original (v1.5) MLS data will be provided in many of the comparisons discussed here.

[4] Section 2 gives a detailed description of the MLS measurements, from (Level 1) spectral radiances and residuals to (Level 2) retrievals and characterization of uncertainties. Section 3 provides an array of comparisons between the MLS ozone profiles and other data sources, from both "routinely acquired" satellite measurements and "campaign-related" data sets, geared specifically toward Aura validation. A companion paper by *Jiang et al.* [2007] compares MLS $O_3$ to profiles from ozonesondes and ground-based lidars. *Livesey et al.* [2008] provide another companion paper that focuses on comparisons versus aircraft measurements of ozone and carbon monoxide in the lowest altitude region, from about 100 to 320 hPa. Several other recent references lend support to the data quality of MLS ozone, mainly for the previous data version (v1.5). In particular, there have been comparisons between MLS and ground-based microwave ozone profiles from Switzerland [*Hocke et al.*, 2007], and analyses by *Ziemke et al.* [2006] and *Yang et al.* [2007], focusing on stratospheric columns and tropospheric ozone residual columns, combining results from MLS and the Ozone Monitoring Instrument (OMI), also aboard Aura. In recent work, *Schoeberl et al.* [2007] use a trajectory-based analysis and OMI and MLS ozone, thus leading to a fine horizontal resolution view of tropospheric ozone residual columns. Comparisons by *Barret et al.* [2006] of v1.5 MLS ozone with ozone retrieved from 500 GHz observations by the Submillimetre Radiometer (SMR) aboard the Odin satellite demonstrate good (~10%) agreement from about 50 to 0.5 hPa. In this special issue, MLS ozone validation analyses are also provided from column comparisons between MLS and measurements obtained during Aura Validation Experiment (AVE) campaigns by the Cavity Flux Spectrometer (CAFS) experiment [*Petropavlovskikh et al.*, 2008], as well as from MLS profile comparisons with ground-based microwave data from New Zealand and Hawaii [*Boyd et al.*, 2007]. In addition, *Manney et al.* [2007] present a broad range of comparisons

**Table 1.** Meaning of Bits in the Status Field

| Bit | Value[a] | Meaning |
|---|---|---|
| 0 | 1 | Flag: Do not use this profile (see bits 8–9 for details). |
| 1 | 2 | Flag: This profile is "suspect" (see bits 4–6 for details). |
| 2 | 4 | Unused |
| 3 | 8 | Unused |
| 4 | 16 | Information: This profile may have been affected by high altitude clouds. |
| 5 | 32 | Information: This profile may have been affected by low altitude clouds. |
| 6 | 64 | Information: This profile did not use Goddard Earth Observing System Model version 5 temperature a priori data. |
| 7 | 128 | Unused |
| 8 | 256 | Information: Retrieval diverged or too few radiances available for retrieval. |
| 9 | 512 | Information: The task-retrieving data for this profile crashed (typically a computer failure). |

[a]Status field in L2GP file is total of appropriate entries in this column.

between various MLS data products, including ozone, and solar occultation data, with a focus on comparisons using equivalent latitude and potential temperature coordinates.

## 2. MLS Measurements

[5] After a brief review of MLS and its measurements (section 2.1), we present typical Level 1 radiance spectra and residuals in section 2.2. Section 2.3 summarizes the data usage and screening recommendations for MLS v2.2 ozone profiles, based on analyses of reprocessed MLS data available at the time of writing, and as used in this work. Sections 2.4 and 2.5 provide a description of estimated MLS ozone uncertainties, both random and systematic, which we refer to as precision and accuracy. Section 2.6 discusses the changes from v1.5 to v2.2, both in the retrieval approach and in the average abundances, as well as the estimated precision and actual scatter in the profiles.

### 2.1. Overview

[6] MLS measures millimeter and submillimeter emission by scanning the Earth's atmospheric limb every 24.7 s ahead of Aura, in a sun-synchronous near-polar orbit with ~13:45 LT ascending equatorial crossing time, thus providing retrievals of daytime and nighttime profiles roughly every 165 km along the suborbital track. The instrument uses five broad spectral regions between 118 GHz and 2.5 THz, covered by seven radiometers. For an overview of the MLS instrument, observational characteristics, spectral bands, main line frequencies, and target molecules, see *Waters et al.* [2006]. Vertical scans are synchronized to the Aura orbit, leading to retrieved profiles at the same latitude every orbit, with a spacing of 1.5° great circle angle along the suborbital track; the 240 limb scans per orbit provide close to 3500 profiles per day, stored in Level 2 data files, in Hierarchical Data Format (more specifically, of the HDF-EOS 5 format type). The vertical retrieval is on a pressure grid with 6 levels (or pressure surfaces) per decade change in pressure in the stratosphere, and with 3 levels per decade for pressures smaller than 0.1 hPa. MLS data from version 1.5 (v1.5) and the recent version 2.2 are available from the NASA Goddard Earth Sciences (GES) Data and Information Services Center (DISC), at http://disc.gsfc.nasa.gov/Aura/MLS/index.shtml. Public information about MLS and MLS data access can be found at the MLS website (http://mls.jpl.nasa.gov).

[7] The radiometric and spectral performances of the GHz radiometers are discussed by *Jarnot et al.* [2006]. The MLS retrieval approach is given by *Livesey et al.* [2006] and the calculation specifics of the MLS radiance model (or "forward model") are described by *Read et al.* [2006] and *Schwartz et al.* [2006]; line of sight gradients are taken into account in these retrievals. Section 2.6 provides information on the retrieval changes that have affected the v2.2 ozone results.

### 2.2. Radiance Spectra and Residuals

[8] MLS retrievals of stratospheric and mesospheric $O_3$ come largely from rotational emission lines in band 7 of the R3 radiometer, which also covers CO as a target gas. Calculated spectra for the whole frequency range (all MLS radiometers) are shown by *Read et al.* [2006]. Typical radiance spectra and accompanying residuals are shown in Figure 1 for the main target $O_3$ line at 235.71 GHz (forming a "lower sideband" contribution to the signal, see the frequency label A) and the nearby line at 243.45 GHz (providing an "upper sideband" contribution, see label B); the two sidebands are combined into the measured "double sideband" radiances. The line wing component of emission arising from the 244.16 GHz line (in the upper sideband) is also evident (see label C) in the spectra of Figure 1, which shows radiances for various tangent heights, from the upper troposphere (near 10 km) to the upper stratosphere (near 50 km), where the lines are much narrower; the band 7 mesospheric retrievals rely mainly on the narrow digital autocorrelator spectrometer (DACS) channels near the ozone line center. The residuals are obtained by differencing the calculated (forward model) average radiances from the measured average radiances arising from 1 d of profiles (trace gases and temperature) retrieved by the MLS v2.2 algorithms. The same residual patterns are evident if we use the same day, but 1 year apart. Typical average residuals in Figure 1 are a few tenths of 1 K to slightly above 1 K. This compares to signal strengths (spectral contrast above the baseline being important here) of order 50–100 K, so the stratospheric residual errors are ~1%. Such good retrieval closure is typically obtained by MLS, with remaining small radiance differences expected to contribute only in a small way to errors in the retrieved product. On the basis of radiance noise of 0.4 to 1.6 K for individual measurements from this band [*Waters et al.*, 2006], the expected precision for daily averages (with more than 3000 spectra per day at each height) is less than 0.1 K. There is therefore a small but systematic component in these residuals (typical of other days' results), and reducing such

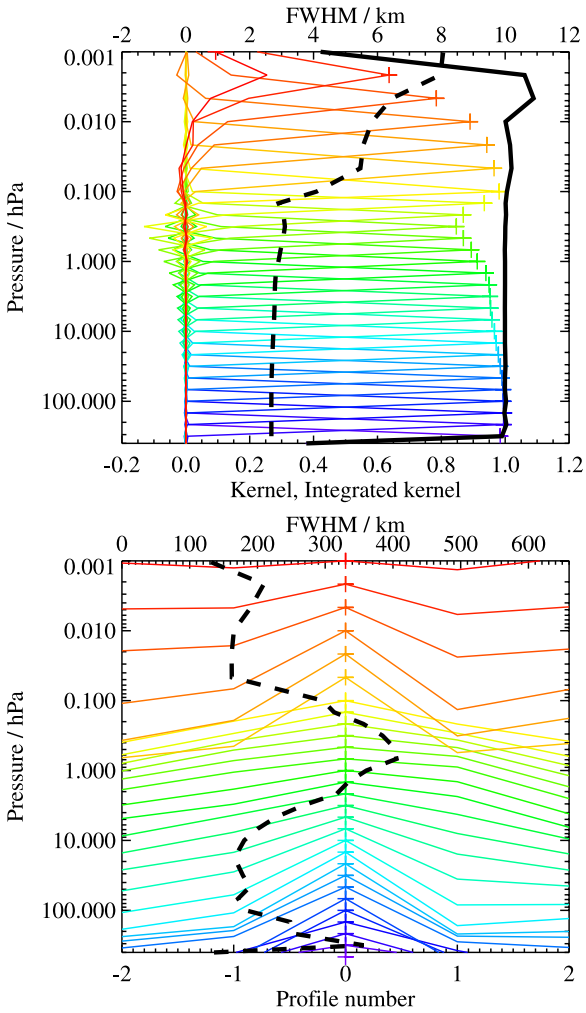


**Figure 3.** (top) Colored lines show typical v2.2 MLS ozone vertical averaging kernels (here for 35°N) as a function of the retrieval level, indicating the region from which information is contributing to the measurements on the individual retrieval surfaces, denoted by plus signs. Kernels are integrated in the horizontal dimension for five along-track scans. The dashed black line is the full width at half maximum (FWHM) and indicates vertical resolution, as given above the top axis. The solid black line shows the integrated area under each of the colored curves. (bottom) Horizontal averaging kernels (integrated in the vertical dimension), with dashed black line giving horizontal resolution (see top axis). The averaging kernels are scaled such that a unit change corresponds to 1 decade in pressure. Profile numbers along the MLS orbit track are given on bottom axis, with profile zero at the tangent point and negative values indicating the satellite side; profile spacing is 1.5° great circle angle, or about 165 km, along the orbit track.

systematics, especially at the lowest altitudes, is a desired task for a future MLS retrieval version.

[9] A pressure/latitude contour plot of typical daily zonal mean "chi square" values for the ozone band (band 7) is shown in Figure 2 (top); these values provide an average representation of the sum of the squared radiance residuals divided by the square of the estimated radiance errors for each tangent viewing location. The median values (not shown) are typically between 1 and 2, but the average values are affected by a limited number of larger values representing poorer fits and/or fewer radiances, especially in the upper troposphere and at tropical latitudes. Figure 2 (bottom) shows a related plot versus latitude for the "Quality" field, stored in the MLS Level 2 ozone files. Quality gives a simple (one number per profile) measure of radiance fits based on the overall chi square, and is directly related to the combination of radiance chi square values for each profile. This plot shows that minima in Quality (the poorest Quality profiles) occur in latitudinal regions with the highest zonal mean values of chi square, and that the largest chi square values occur at the lowest altitudes. As done for v1.5 data [*Livesey et al.*, 2005], we recommend (see next section) a Quality threshold for data screening.

### 2.3. Data Usage and Screening

[10] The recommendations below for screening the MLS ozone profiles are similar to those given for version 1.5 data [see *Livesey et al.*, 2005]. However, there are slightly different threshold values for v2.2, because of some rescaling of the relationship between radiance fits and Quality, and there is a new flag ("Convergence") to take into account.

#### 2.3.1. Status Field

[11] As for v1.5 data, ozone profiles should be used if the field named "Status" has an even value; this field will have an odd value if the retrieval diverged or not enough radiances were used, or some other anomalous instrument or retrieval behavior occurred. The retrieved profile may be considered "questionable" if Status is even but nonzero, in particular if clouds may have affected some of the tangent views for a particular profile's retrieval. However, we see no evidence to recommend an outright rejection of all profiles with such questionable Status values (affecting 10–15% of the daily MLS profiles), having inspected how these questionable profiles compare to others at similar latitudes. Table 1 summarizes the various bit values that can affect the value of Status.

#### 2.3.2. Quality Field

[12] As mentioned in the previous section, the Quality field in the Level 2 ozone files can discriminate retrieved profiles that have poor radiance fits, although no specific information is provided about which height(s) exhibit the worst fit, unless one inspects the height dependence of radiance chi square values in the MLS Level 2 "DGG" files. The poorest fits exist at the lowest altitudes and often in the tropics, possibly in relation to cloud-related effects on the MLS radiances. We recommend use of stratospheric ozone profiles with Quality >0.4, in order to screen out the poorest radiance fits (typically ~1% of available daily profiles and a few % at low latitudes). We note that a tighter criterion (Quality >1.2) is recommended for the upper troposphere [*Livesey et al.*, 2008], meaning primarily for low latitude regions at pressures of 100 hPa or more.

#### 2.3.3. Convergence Field

[13] This is a new (version 2.2) field in the L2GP files, and it refers to the ratio of chi square value, from radiance fits for each "chunk" of typically ten profiles, to the value that the retrieval would have been expected to reach. Since we have not generally observed anomalous behaviors for

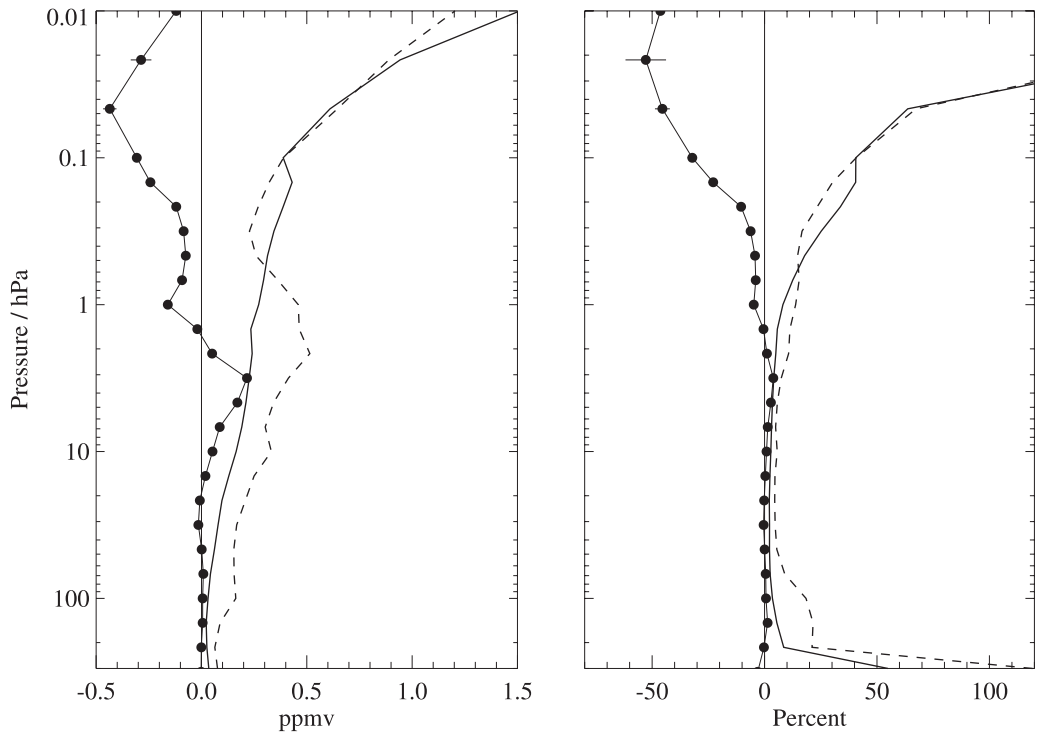


**Figure 4.** The estimated single-profile precision as a function of pressure for a typical day of MLS data (here for June 15, 2005) is shown as the solid line (with no dots), based on the root-mean-square (RMS) of MLS retrieval uncertainty estimates (see text), using the 741 matched profile pairs mentioned below. An empirical estimate of precision (repeatability) is given by the dashed line, corresponding to the RMS scatter (divided by square root of 2) about the mean differences, for all near coincidences using both ascending and descending MLS profiles (741 matched profile pairs, using a 300 km distance matching criterion). The mean differences are given by the line connected with dots, with error bars (often smaller than the dots) giving the precision (standard error) for these mean differences. Diurnal changes in ozone cause the large mean differences in the mesosphere.

the profiles with larger than average values of Convergence, a field with values between 1 and 1.1 for the vast majority of profiles, we recommend use of ozone profiles with Convergence <1.8. This eliminates a very small fraction of the available ozone profiles, as many days do not have any such profiles; on occasion, a few profile chunks get flagged by such a Convergence value.

#### 2.3.4. Precision Values

[14] As for v1.5 data, we recommend that users ignore the ozone values at pressures where the estimated precision is flagged negative, typically only for 0.01 hPa and lower pressures; this happens where the influence of the a priori becomes large, specifically where the estimated precision divided by the a priori uncertainty is larger than 0.5. Pressures (in the mesosphere and troposphere) where the precision values do provide a data screening criterion generally occur at a fairly sharp transition between good and poor MLS sensitivity, although there is still some MLS sensitivity in the uppermost mesosphere, for example, if one uses average abundances.

#### 2.3.5. Vertical Range

[15] Our analyses of MLS sensitivity and precision, coupled with the characterization and validation studies described here and in related upper tropospheric analyses [*Livesey et al.*, 2008], lead us to recommend that only MLS ozone values from 215 to 0.02 hPa be used. The 147 and 215 hPa MLS levels generally lie in the upper troposphere at low latitudes, but can be in the stratosphere at high latitudes. The limit at 0.02 hPa is a conservative single-profile sensitivity limit, although studies of ozone at higher altitudes may be performed, with caution (and preferably in consultation with the MLS team).

[16] In summary, data users should only use MLS ozone profiles from 215 to 0.02 hPa with (1) even value of Status, (2) positive precision values, (3) Quality value > 0.4 (with a higher cutoff value of 1.2 for 100 to 215 hPa), and (4) Convergence value < 1.8. These criteria will allow for the reliable use of more than ~97% of available daily MLS $O_3$ profiles, with the precision and accuracy described later in this work being applicable.

### 2.4. Precision and Resolution

[17] The MLS antenna field of view for the 240 GHz radiometer has a width of 3.2 km at the limb tangent point in the vertical direction, and 6.4 km in the horizontal (across-track) direction [*Waters et al.*, 2006]. The measurement resolution is also affected by the radiative transfer averaging path through the atmosphere. The resolution, both vertical and along the MLS suborbital track, can be visualized through the use of the averaging kernel matrix, as described for atmospheric retrievals by *Rodgers* [1976]. Figure 3 displays vertical and horizontal averaging kernels for a typical MLS ozone retrieval at 35°N; different latitudes give very similar results. We note that the averaging

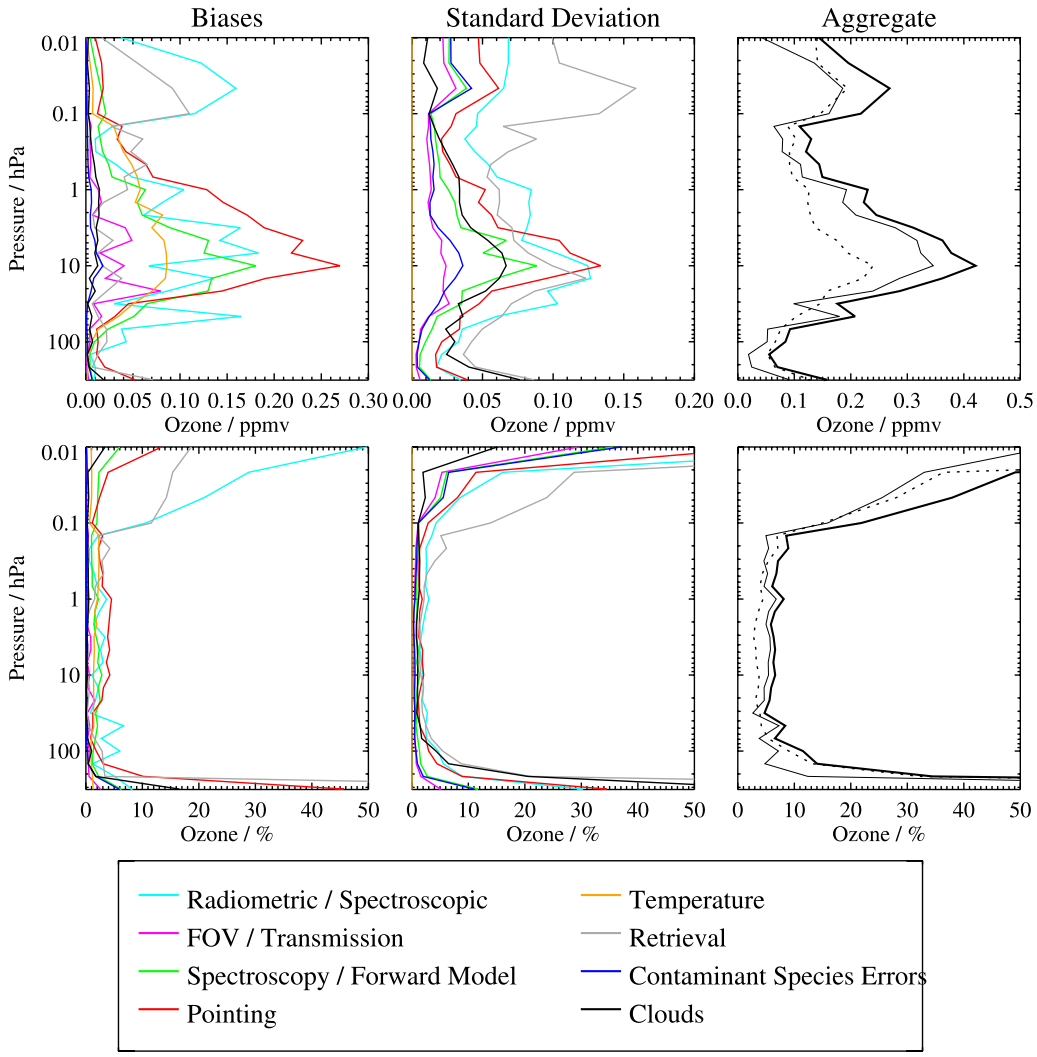


**Figure 5.** Estimated impact of various families of possible systematic errors on the MLS ozone observations. (left) Possible magnitudes of the biases and (center) additional RMS scatter introduced by the various families of errors, with each family denoted by a different colored line. Cyan lines denote errors in MLS radiometric and spectral calibration. Magenta lines show errors associated with the MLS field of view and antenna transmission efficiency. Red lines depict errors associated with MLS pointing uncertainty. The impact of possible errors in spectroscopic databases and forward model approximations are denoted by the green line, while those associated with retrieval formulation are shown in gray. The gold lines indicate possible errors resulting from errors in the MLS temperature product, while the blue lines show the impact of likely errors in other species. Finally, the typical impact of cloud contamination is denoted by the black line. (Right) The root-sum-squares (RSS) of all the possible biases (thin solid line), all the additional RMS scatter (thin dotted line), and the RSS of the two (thick solid line).

kernels' peak values are near unity from 316 to 0.01 hPa; there is negligible influence on the retrievals in this region from our choice of a priori values and uncertainties, as confirmed by sensitivity tests. The retrieval grid changes to a coarser grid for pressures lower than 0.1 hPa, as indicated in Figure 3 (top), and the vertical resolution degrades accordingly; the horizontal resolution in that region does improve, as indicated by Figure 3's (bottom) averaging kernel widths, as a result of a better discrimination of this dimension given the coarser vertical spacing. The more highly peaked horizontal averaging kernels in the 10 to 100 hPa region arise from the ozone signal being spread out across more channels. Figure 3 also depicts (as thick dashed black lines) the vertical and horizontal resolution, using the half width at full maximum of the averaging kernels as a measure. The vertical resolution is ~2.7 to 3 km from the upper troposphere to the midmesosphere, and the horizontal resolution is mostly between 200 and 300 km.

[18] The precision of the ozone measurements can be arrived at from the uncertainties that are estimated by the MLS retrievals, following the general *Rodgers'* [1976] formulation [see *Livesey et al.*, 2006]; precision values are provided in the MLS Level 2 files as the diagonal values of the error covariance matrix. Figure 4 shows typical values of this estimated precision, along with an empirical estimate from root-mean-square (RMS) scatter about the mean for

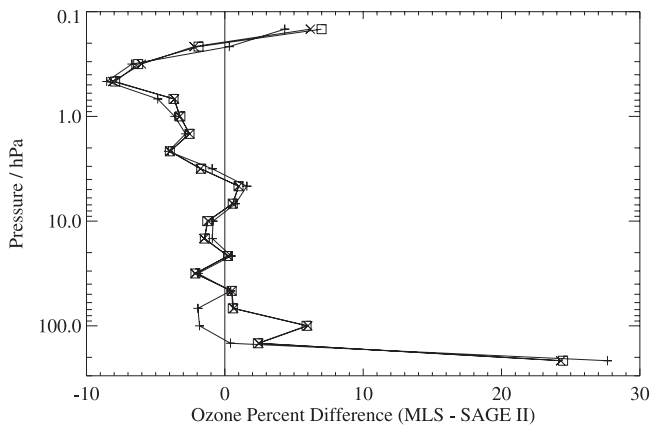


**Figure 6.** Sensitivity of profile differences (v2.2 MLS data minus v6.2 SAGE II data, expressed as a percent of SAGE II averages) to the treatment of SAGE II profiles, coincident with the MLS profiles, for an averaged set of 1310 matched profiles (throughout the globe) from about 50 available days between September 2004 and August 2005. Plus signs represent a simple interpolation method versus log of pressure, crosses are from a least squares fit of the SAGE II profiles to the MLS retrieval grid, and the open boxes give the result after adding the smoothing effect of the MLS vertical averaging kernels; the latter results are very close to the simpler least squares formulation, given the generally nicely peaked nature (and near-unity value) of the MLS-averaging kernels.

matched profile pairs from the ascending and descending portions of the orbit. Note that this scatter has been reduced by square root of two in the plot shown here, since the scatter between ascending and descending profiles should be larger, by this factor, than the individual precision. The maximum distance separating ascending and descending profiles selected here is 300 km. This scatter between ascending and descending profiles is quite similar to the RMS scatter within a narrow latitude bin where atmospheric variability is expected to be small (e.g., 5°S to 5°N in the middle stratosphere). The precision obtained from the scatter in (ascending versus descending) MLS profiles is most often larger than the estimated precision in the stratosphere and upper troposphere, as atmospheric variability adds some scatter. The scatter is also sometimes somewhat less than the precision, as can be observed for the mesosphere; this is a result of the retrieval a priori influence and smoothing constraints, even though there is no smoothing constraint for pressures less than 0.1 hPa. The mean differences between ascending and descending profiles (shown as dots in Figure 4) are typically very small in the stratosphere, but there are significant differences in the upper stratosphere and mesosphere, due to diurnal variation at these heights.

[19] The estimated RMS precision (from the MLS Level 2 files) can be as low as 30 ppbv from 100 to 215 hPa, and increase to 0.3 ppmv near 1 hPa. Although the precision is fairly constant versus latitude, there can be variations of a factor of two, especially at the lower altitudes, between equatorial and polar regions.

[20] The precision in MLS column abundances down to pressures of 100 to 215 hPa is 2–4 Dobson units (DU), or ~2%, based on an analysis of simulated retrievals. Comparisons of actual MLS profiles from ascending and descending sides, as well as tropical measurement variability, lead to 3% as a conservative estimate for the precision of the MLS columns.

### 2.5. Expected Accuracy

[21] Comparisons with well-characterized and accurate data can provide valuable information about possible systematic uncertainties (see section 3); so can an assessment of known or potential error sources, discussed here. Systematic errors arise from instrumental effects such as imperfect radiometric calibration or field of view characterization, as well as from errors in laboratory spectroscopic data, or retrieval formulation and implementation. This section summarizes our quantification of these errors for ozone. Details of this assessment approach are provided by *Read et al.* [2007].

[22] For each source of systematic error, the impact on the MLS radiance measurements (or pointing, where appropriate) has been quantified and modeled. These modeled effects correspond to either 2 sigma estimates of uncertainty in the modeled quantity, instrument calibration uncertainty, or the sensitivity to a priori. The impact of these perturbations on retrieved products has been quantified by one of two methods. In the first method, modeled errors have been applied to simulated MLS radiances, based on a model atmosphere, for a whole day of MLS observations. These perturbed radiances have then been run through the routine MLS data processing algorithms, and the systematic errors have been evaluated from the impact of the perturbation on the Level 2 products (i.e., the resulting differences from an "unperturbed" run). In addition to giving an estimate of any bias introduced by the various error sources, these "full up" studies also quantify any additional scatter (standard deviation about the mean bias) introduced in the retrievals by each error source. The difference between the retrieved product in the unperturbed run and the original "true" model atmosphere is taken as a measure of errors due to retrieval formulation and numerics; bias magnitudes from various error sources (tests) are obtained by combining average differences from different tests in root sum square fashion. The impact of some systematic errors has been quantified through analytic calculation based on simplified models of the MLS measurement system [*Read et al.*, 2007]. Figure 5 gives the impact on ozone from a number of error sources, as well as the combined (root-sum-square (RSS)) results. There are possible biases of 0.05 to 0.3 ppmv for most of the stratosphere (100 to 1 hPa), with total errors (including the random component) of ~5–10%. The bias (typically under 7% in this region) is the error one might expect to see in a multiprofile comparison versus true profiles, whereas the total uncertainty is more relevant for single profile comparisons, as it includes a random component. Accuracy estimates have also been made in terms of multiplicative terms and additive biases, as discussed for the lower altitudes by *Livesey et al.* [2008]. The percent uncertainties increase at higher pressures, as ozone values become small in the tropics and upper troposphere.

[23] Especially in the lower stratosphere, the Aura MLS ozone uncertainties are significantly smaller than those of UARS MLS, estimated at ~0.3 ppmv [*Froidevaux et al.*, 1996], primarily because of the wider bandwidth of the

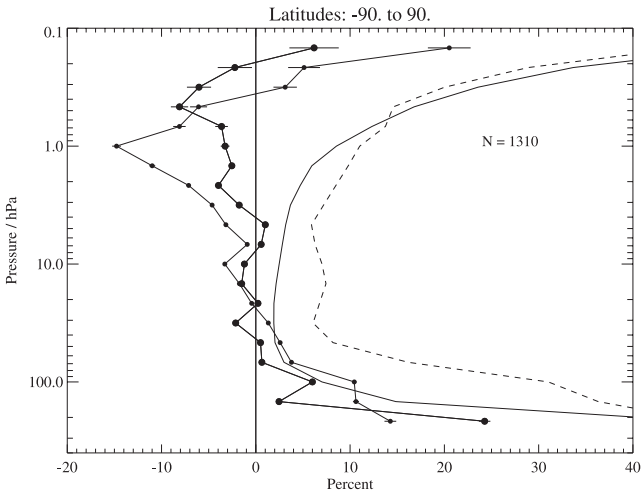


**Figure 7.** Global average ozone differences for MLS – SAGE II (with respect to SAGE II averages), based on coincident profiles obtained from about 90 d of version 2.2 MLS data in 2004 and 2005 (and for 1310 matched profile pairs, as indicated by number *N* above); see text for coincidence criteria used. The large connected dots are for MLS v2.2 data (same result as the crosses shown in Figure 6), whereas the small dots are for v1.5 MLS data. Error bars on these dots represent twice the standard error of the mean differences. The dashed line gives the standard deviation of the differences, and the solid line is an estimate (see text) of the combined precision (random error) of the two measurements.

Aura MLS spectrometers. Results in Figure 5 and from other analyses (not shown) of the individual components contributing to each of these families of lines [*Read et al.*, 2007] show that the major contributors to the ozone uncertainty are from (1) pointing-related uncertainties (red lines), (2) radiometric and spectral calibration (cyan lines), and (3) retrieval formulation (gray lines). Ozone spectroscopic error contributions, the largest component of the values shown by the green lines, are not a major fraction of the total errors, which means that large improvements in ozone accuracy are not expected from better spectroscopic knowledge at 240 GHz, where the linewidth is estimated to have a 3% uncertainty; the oxygen line width uncertainty (also 3% [see *Read et al.*, 2007]) contributes to pointing uncertainty as well, but only as roughly one third of the total. Finally, we note that cloud-related errors (black lines) do not contribute much to the total error; this adds confidence to our recommendation not to discard MLS ozone profiles that may be in the vicinity of clouds, as determined by MLS "window channel" radiances [*Wu et al.*, 2008] and flagged using MLS ozone Status values.

[24] The expected accuracy in the column abundances, using MLS ozone profile integrations down to pressures of 100 to 215 hPa, has also been assessed from the sensitivity analyses mentioned above. We find that the (2 sigma) accuracy estimate for columns arising from the integration of MLS ozone profiles down to pressure levels of 100 to 215 hPa is about 4%.

### 2.6. Differences Between v2.2 and v1.5 Data

[25] Version 2.2 differs from version 1.5 mainly because of indirect effects from the coupled retrievals of temperature and tangent pressure [see *Schwartz et al.*, 2007]. The use of slightly different bands and channels, as well as some calibration corrections for the digital autocorrelator spectrometer (DACS) channels used in these retrievals, have led to slightly lower MLS temperature retrievals, and a related shift in tangent pressure, increasing from near zero in the lower stratosphere to the equivalent of a few hundred meters near 1 hPa. Mesospheric ozone changes have also occurred as a result of calibration changes for the DACS channels used in the center of band 7.

[26] The changes in MLS $O_3$ are systematic (e.g., versus latitude), with little change in the scatter or precision of stratospheric or mesospheric $O_3$. Slightly lower abundances are retrieved near 100 hPa, near-zero change occurs at 15–20 hPa, as well as near 0.5 hPa, while larger values (by ~10%) now exist near 1 hPa. Mesospheric values are now lower, with larger departures from v1.5 as height increases, and changes of −10% to −30% in the upper mesosphere. In the tropical upper troposphere, the largest percent difference occurs at 215 hPa, where the new version gives smaller values, and where both values and gradients appear more realistic. Section 3 provides a view of typical percent changes between the two MLS data versions.

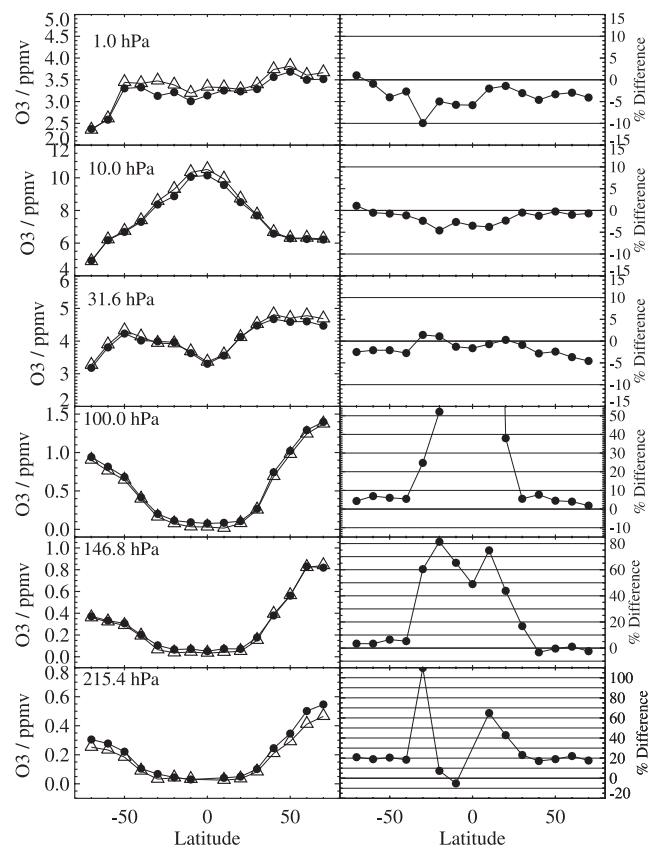


**Figure 8.** (left) Zonally averaged values of ozone versus latitude for coincident measurements from MLS (circles) and SAGE II (triangles) at the pressures indicated in each section. (right) Ozone differences versus latitude for MLS – SAGE II, as a percentage of the mean SAGE II values. The data here apply to all available matched profiles from days reprocessed with MLS v2.2 data, as in Figure 7.

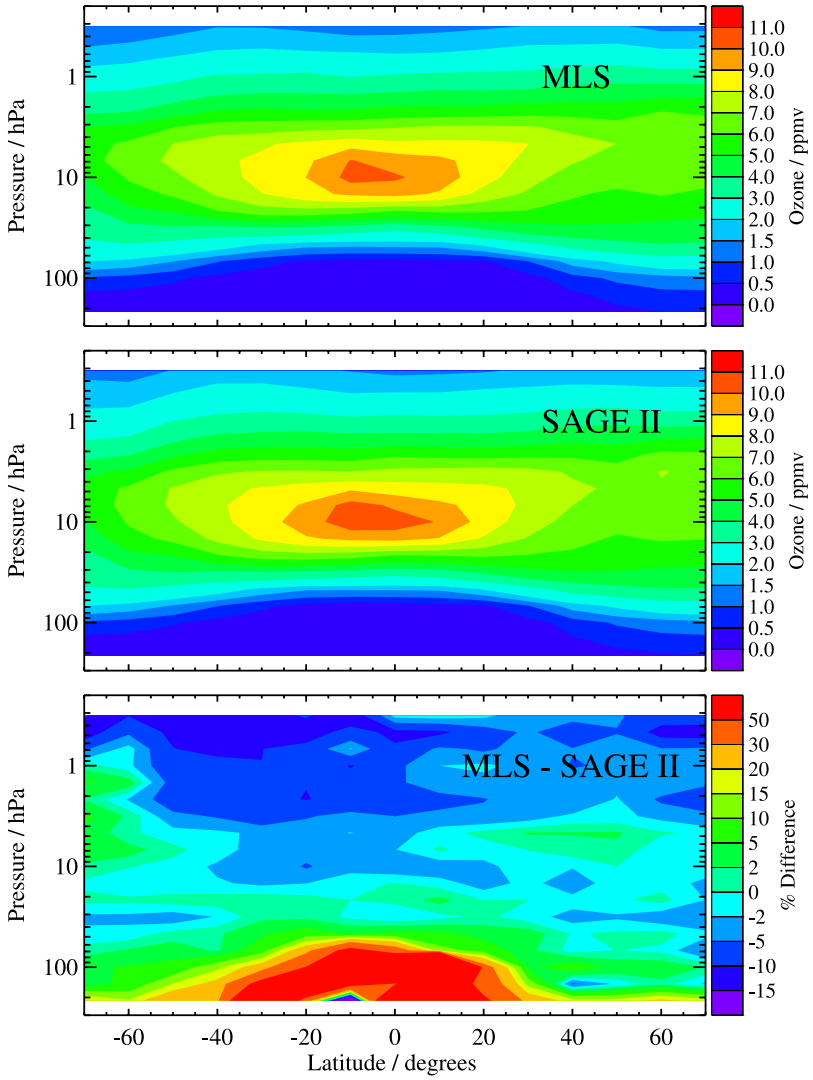


**Figure 9.** (top) Contour plot of zonally averaged v2.2 MLS ozone profiles versus latitude for January–March 2005, including only the coincidences with available SAGE II profiles. (middle) The contour plot for SAGE II profiles that are matched to the MLS profiles. (bottom) Differences MLS – SAGE II, as a percentage of the SAGE II values.

[27] The changes mentioned above for the MLS profiles have led to a slight reduction in stratospheric column abundances that can be calculated from an integration of the profiles above the tropopause, or in column abundances down to pressures larger than (or equal to) 100 hPa. As mentioned by *Yang et al.* [2007], some compensation occurs from higher altitudes, where MLS ozone values have increased by a few to 10%. Depending on the lower pressure level used for column integrations (from 100 to 215 hPa), the v2.2 MLS column abundances are ~0.5 to 2% (typically 1 to 4 DU) smaller than the v1.5 values, and the standard deviation of the differences is 4 to 5%.

## 3. Comparisons With Other Data Sources

### 3.1. Comparisons With Satellite Data

#### 3.1.1. MLS and SAGE II Profiles

[28] The SAGE II ozone profiles, measured via solar occultation at wavelengths near 600 nm, with a vertical resolution of about 1 km, have been validated extensively [*H.-J. Wang et al.*, 2002; *P.-H. Wang et al.*, 2006] and have provided one of the best available data sources (in combination with SAGE I data) for studying long-term trends [e.g., *World Meteorological Organization*, 2003; *Yang et al.*, 2006]. We should therefore be able to rely on comparisons with SAGE II to ascertain the quality of MLS stratospheric $O_3$. Comparisons with SAGE III are not given here, but analyses by *H.-J. Wang et al.* [2006] have shown that SAGE III $O_3$ results do not differ much from SAGE II, with SAGE III typically giving larger values by a few to 5%. Also, SAGE III solar occultation profiles are limited to high latitudes. Good agreement between v1.5 MLS and SAGE III profiles is discussed by *Yang et al.* [2007] and by *Manney et al.* [2007], for MLS v2.2 data.

[29] We first illustrate the effects of interpolation and smoothing methods on the comparisons. The MLS retrieval system assumes a piecewise linear representation of the atmospheric state versus log (pressure), as provided by

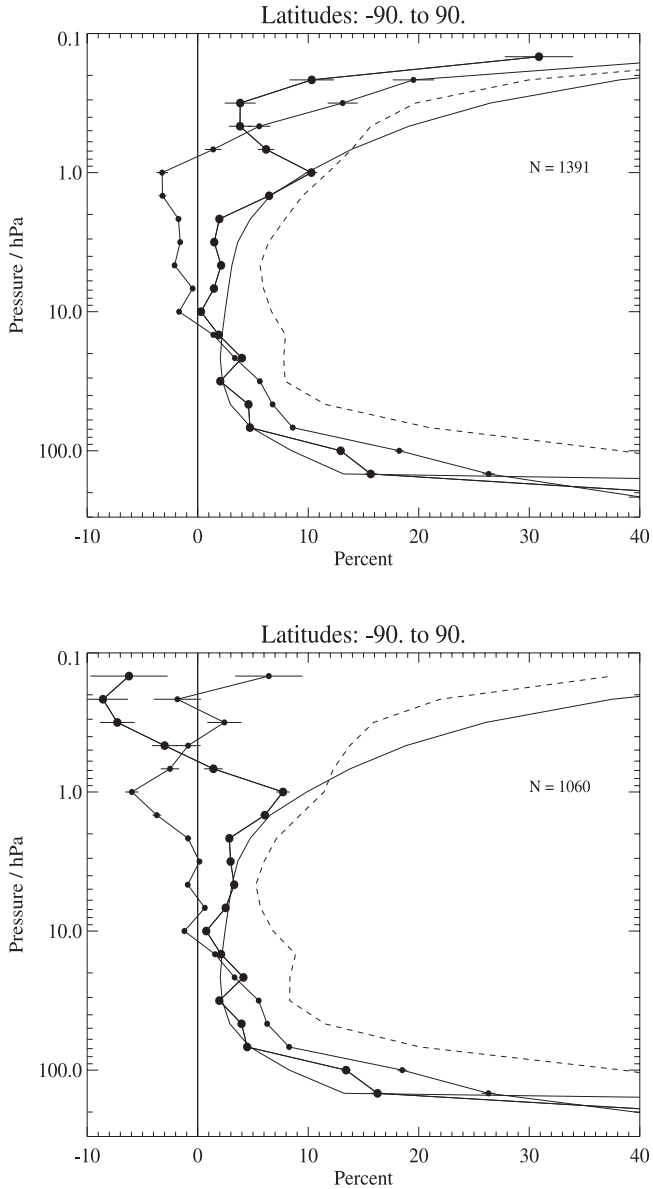


**Figure 10.** (top) Same as Figure 7 but for MLS and HALOE (version 19) ozone differences from available matched profile pairs in 2004 and 2005. (bottom) Same as Figure 10 (top) but using MLS daytime observations only.

simple triangular basis functions $\eta$, with unit value at a given retrieval grid point, and decreasing linearly to zero at the adjacent (log pressure) levels; a fine-resolution representation ($x_{\mathrm{fine}}$) can be obtained by multiplying the discrete state vector ($x_{\mathrm{coarse}}$) by the matrix of basis functions, so that $x_{\mathrm{fine}} = \boldsymbol{\eta}\, x_{\mathrm{coarse}}$. As discussed by *Read et al.* [2006], a least squares fit method of smoothing a fine-resolution correlative profile ($x_{\mathrm{correl}}$) can be used for comparisons with MLS; solving the previous equation for $x_{\mathrm{coarse}}$ leads to $x_{\mathrm{coarse}} = [\boldsymbol{\eta}^{\mathbf{T}}\ \boldsymbol{\eta}]^{-1}\ \boldsymbol{\eta}^{\mathbf{T}}\ x_{\mathrm{correl}}$. In Figure 6, we compare average results between available SAGE II and MLS profiles (1310 matched profiles), using three methods for transforming the finer vertical resolution SAGE II profiles onto the MLS retrieval grid: simple interpolation versus log (pressure), least squares fit as defined above, and an additional smoothing using the MLS vertical averaging kernel matrix **A** (section 2.4). The latter method follows *Rodgers* [1976] and *Rodgers and Connor* [2003] to get $x_{\mathrm{smooth}} = x_a + \mathbf{A} \cdot (x_{\mathrm{coarse}} - x_a)$, a smoothed version of the correlative data profile. We transform the correlative data precisions in the comparisons given in this paper by using interpolation versus log (pressure), for simplicity, as these values do not influence the results in a significant way. Figure 6 provides the average percent differences between available MLS v2.2 and coincident SAGE II (version 6.2) profiles, with coincidence defined in this paper (unless otherwise specified) as within ±2° latitude, and ±8° longitude, on the same day. SAGE II ozone mixing ratios versus pressure are readily obtained from the SAGE II files (with ozone and air concentrations as a function of pressure). Differences of only a few % among the 3 methods exist for pressures less than 100 hPa, with somewhat bigger differences observed at larger pressures, where simple interpolation can sometimes lead to the best agreement, even if this may be coincidental. The larger values near 100 hPa for the least squares and averaging kernel smoothing methods arise because of the way the smoothing process "negotiates" sharp gradient changes that often occur there; the resulting smoothed SAGE II data near 100 hPa are most often lower than the finer resolution profile values, and the differences (MLS – SAGE II) are therefore larger than obtained via linear interpolation.

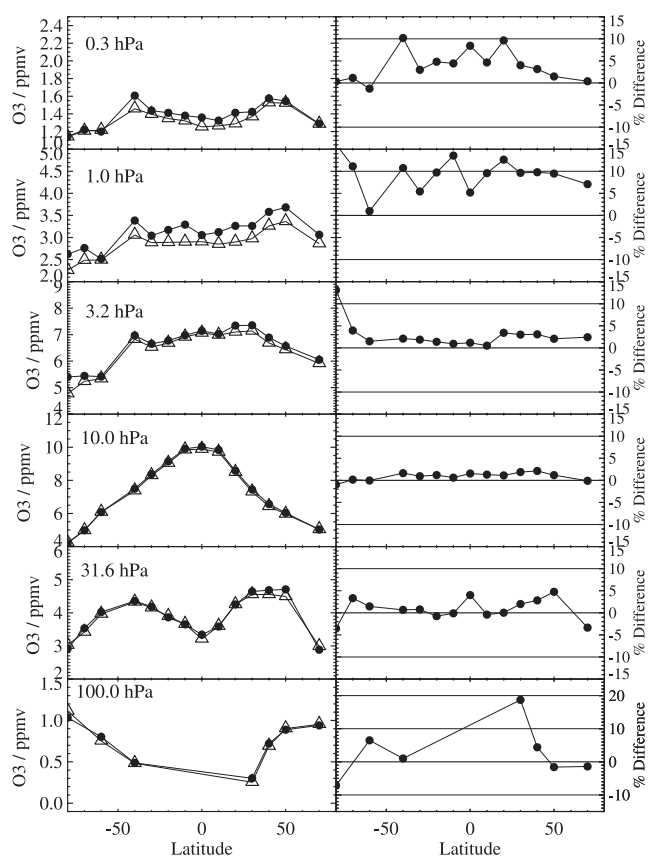


**Figure 11.** Same as Figure 8 but for MLS and HALOE ozone comparisons.

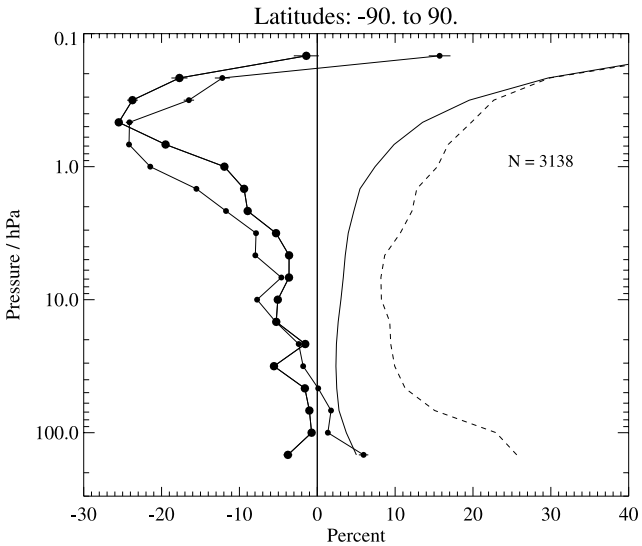


**Figure 12.** Same as Figure 7 but for MLS and ACE-FTS (version 2.2 ozone update) differences (for 3138 available matched profile pairs in 2004, 2005, and 2006).

[30] The difference results for MLS versus SAGE II profiles, smoothed using the least squares fitting method, are repeated in Figure 7, along with a comparison of the standard deviations of the differences and the combined precisions, the latter being obtained from the RSS of the random profile uncertainties for MLS and SAGE II. The standard deviations of the differences (or "scatter") can be as low as 5% in the stratosphere, with increases at the lowest altitudes reflecting increased atmospheric variability, as the expected combined precisions are lower than the observed scatter. However, tropical latitudes or summer high latitudes (not shown separately here), give somewhat better agreement between expected combined precision and observed scatter in the differences, although this scatter does not dip below 4%. This sensitivity to region/season is also illustrated for MLS and POAM III comparisons in a later subsection, although the impact of such considerations is usually minor, in terms of the observed average differences. We can find better overall agreement between the precisions and the standard deviations if we assume a larger precision for the SAGE II profiles. *Borchi et al.* [2005] estimate that the SAGE II precision is about 2 to 3%, but the uncertainty values from the SAGE II files are often significantly smaller than this, so the combined precisions in Figure 7 are probably an underestimate.

[31] Results of the coincident profile comparisons, binned in 10° latitude bins, are provided in Figure 8. The latitudinal behavior is tracked in a very similar fashion by both sets of data. This is also illustrated in Figure 9, which only uses data from January to March, 2005. The MLS tropical ozone values are larger than the SAGE II values at 100 to 215 hPa, although part of the accentuated percent difference arises from the low ozone values in this region. The average MLS values in this pressure range are about 30 to 90 ppbv in the tropics, compared to 20 to 40 ppbv for SAGE II; the percent differences cover a wide range and can reach 200 to 400% at 100 hPa (not all percent values are shown in Figure 8). Part (but not all) of the upper tropospheric tropical discrepancy arises from SAGE II; indeed, SAGE II ozone has been shown to be low (by as much as 30–50%) versus ozonesonde data below the tropopause [*H.-J. Wang et al.*, 2002; *P.-H. Wang et al.*, 2006], with better (10%) agreement above the tropopause.

### 3.1.2. MLS and HALOE Profiles

[32] In the following comparisons with other satellite instrument data, we use the least squares fit method for smoothing the correlative data sets. Figure 10 shows global percent differences between MLS and HALOE version 19 data; HALOE provides solar occultation infrared measurements [*Russell et al.*, 1993], with a vertical resolution for $O_3$ of ~2 km. Figure 10 shows separate results of the comparisons using day and night MLS profiles (Figure 10 (top)) and daytime only MLS profiles (Figure 10 (bottom)), as mesospheric comparisons require additional care because of diurnal changes in that region. Indeed, *Boyd et al.* [2007] point out that daytime observations should give better agreement with HALOE twilight observations in the mesosphere, which has elevated nighttime ozone; Figure 10 illustrates that this is indeed the case. Ground-based microwave observations should provide the best means of validating the day and night MLS $O_3$, and related variations in the upper stratosphere and mesosphere. *Hocke et al.* [2007] have demonstrated good agreement between MLS and ground-based microwave ozone data from Switzerland. Excellent agreement (most often within 5%) is also found between MLS v2.2 data and ozone from the ground-based microwave measurements at Mauna Loa, Hawaii and Lauder, New Zealand, as discussed by *Boyd et al.* [2007]. We note that HALOE retrievals take into account variations along the line of sight in (twilight) mesospheric ozone, whereas the other satellite occultation instrument retrievals do not; however, the impact of twilight gradients on HALOE mesospheric ozone could still be as large as 20% (for sunrise occultations in particular), if improved treatment of these effects were to be included in the HALOE retrievals [*Natarajan et al.*, 2005]. The stratospheric MLS/HALOE ozone comparisons shown in Figure 10 are slightly poorer than the MLS/SAGE II comparisons, but still very good (within 5% between 68 and 2 hPa), with HALOE values slightly lower than those from MLS. This level of agreement is not surprising, as the SAGE II and HALOE ozone measurements often agree to within about 5%, with HALOE ozone typically also slightly lower than the SAGE II values [e.g., *Nazaryan et al.*, 2005]; however, results of the HALOE/SAGE II comparisons in the latter reference are not given below 20 km. At the largest pressures shown here (100 and 147 hPa), the MLS values are larger than the HALOE values by 15% on average. Figure 11 gives latitudinal comparisons for the matched MLS/HALOE profile pairs and indicates good comparisons at midlatitudes to high latitudes, with larger differences arising at low latitudes, where there are also few coincident profiles. *Bhatt et al.* [1999] have noted that comparisons of ozonesonde profiles versus HALOE data give good results (within about 10%) down to 100 hPa at low latitudes, and down to 200 hPa at extratropical latitudes. However, HALOE tends to show low values versus ozonesondes at the highest pressures, and interference from aerosols or cirrus significantly reduces the number of available profiles for pressures larger than 100 hPa. We observe in Figure 10 that the standard

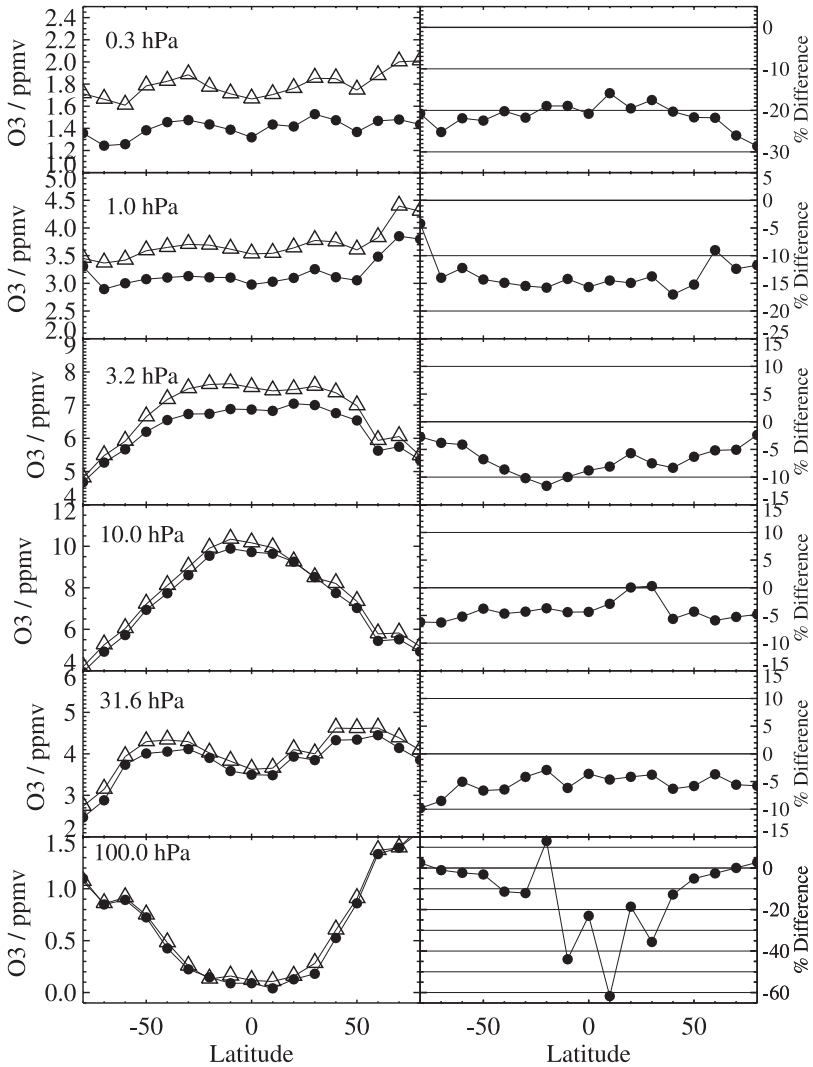


**Figure 13.** Same as Figure 8 but for MLS and ACE-FTS ozone comparisons.

deviation of the differences in the stratosphere can get to within two percent of the estimated combined precision, but is on the high side of this estimate. This is probably for reasons similar to those mentioned for the SAGE II comparisons: imperfect coincidences and real atmospheric variability, and possibly some underestimate of HALOE precision. As for MLS versus SAGE II, there can be variations of 50% or more in the scatter of differences with respect to the (Figure 10) global results, with somewhat better results in the tropics and poorer results in the winter high latitudes.

### 3.1.3. MLS and ACE-FTS Profiles

[33] Figures 12 and 13 show analyses similar to those in Figures 7 and 8, but for MLS versus the Atmospheric Chemistry Experiment Fourier Transform Spectrometer (ACE-FTS) ozone results during 2004 through 2006. ACE-FTS on the SCISAT mission provides retrievals [*Boone et al.*, 2005] since February 2004 for $O_3$ and many other species from solar occultation observations at high resolution (0.02 $cm^{-1}$) in the infrared (2 to 13 $\mu$m). The vertical resolution for $O_3$ is $\sim$ 4 km, with retrievals provided on a 1 km grid; the ACE-FTS version 2.2 ozone "update" is used here, with retrieval "microwindows" only from the 10 $\mu$m spectral region. The MLS/ACE differences in Figure 12 are small (within $\sim$5%) in the lower stratosphere, but increase with altitude and are largest in the upper stratosphere. The MLS results in the latter region agree better with other satellite data sets shown here, as well as with ground-based lidar [*Jiang et al.*, 2007] and microwave [*Hocke et al.*, 2007; *Boyd et al.*, 2007] measurements. The apparent high bias in ACE-FTS upper stratospheric ozone was noticed in v1.0 ACE-FTS data [*Walker et al.*, 2005], and persists in the v2.2 ACE data version, as well as in a sampling of the latest (v3.0) ACE retrievals. Some (maybe most) of this could be caused by the difficulty associated with retrieving at twilight (during solar occultation) when the line of sight gradients in ozone are strong enough to perturb retrievals that assume a homogeneous atmosphere. The standard deviations of the differences in Figure 12 are, as in the previous comparisons versus SAGE II and HALOE, an upper limit for the estimated combined precision; this scatter in the differences can be as low as 5% in the middle stratospheric tropics, for example. The latitudinal variations of these coincident (and averaged) profiles

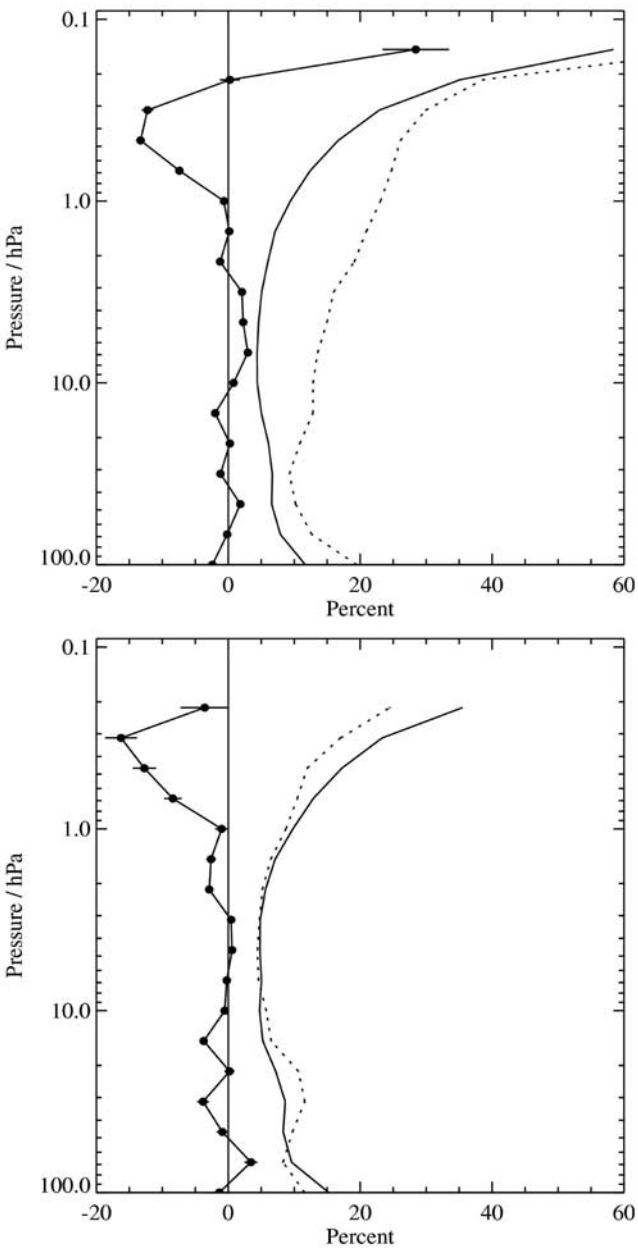


**Figure 14.** (top) Same as Figure 7 but for MLS (version 2.2) and POAM III (version 4) comparisons from 2004, 2005, and 2006 data (691 matched profile pairs). (bottom) This comparison is for a subset of the MLS and POAM III data (94 profile matches), showing the impact of using only September 2005 data (Northern Hemisphere).

agree quite well, as shown in Figure 13; this is also demonstrated, as a function of equivalent latitude, by *Manney et al.* [2007].

### 3.1.4. MLS and POAM III Profiles

[34] We also compare MLS ozone versus the high latitude measurements from POAM III, which uses solar occultation observations at UV/visible wavelengths to provide ozone profiles with a vertical resolution of about 1 km; version 4 POAM III data are used here. Previous validation studies have documented POAM III stratospheric ozone data as being of high quality; [see *Randall et al.*, 2003; *Lumpe et al.*, 2003]. The MLS/POAM III comparisons in Figure 14 show better than 5% agreement on average, from 100 to 1 hPa. Comparisons in the mesosphere are slightly poorer, in terms of average percent differences, but this region is complicated by diurnal changes and the potential for larger solar occultation retrieval errors caused by rapidly changing ozone along the line of sight. Figure 14 (top) gives results using all available MLS and POAM III latitudes and seasons, whereas Figure 14 (bottom) illustrates the changes obtained when using a smaller subset of data, in this case, September 2005. There are still nearly 100 coincident profiles used for the latter case, and the average differences are very similar to those obtained with the expanded data sets (Figure 14 (top)). However, the smaller subset uses only Northern Hemisphere occultations during a month with less atmospheric variability than during the polar winter months; as a result, the standard deviation of the differences between MLS and POAM III is reduced and essentially the same as expectations from the combined precisions. This confirms that comparisons that include profiles in regions of large spatial (and/or temporal) gradients will be affected by such conditions, although mostly in the scatter of the differences. The MLS comparisons versus SAGE II and HALOE suffer less from such an issue because of the "dilution effect" from a number of (matched) profiles outside of high latitude winter conditions.

[35] We note that the average differences in Figure 14 exhibit oscillations in the lower stratosphere, with a positive "notch" at 22 hPa, for example. Such an effect is also apparent, while subtle, in the earlier plots of MLS global differences versus SAGE II (Figure 7), HALOE (Figure 10), and ACE-FTS (Figure 12). The oscillations are observed more easily where the ozone vertical gradients are shallower, at high latitudes in particular (plots not shown here). These small oscillations (of order 5%) seem to generally

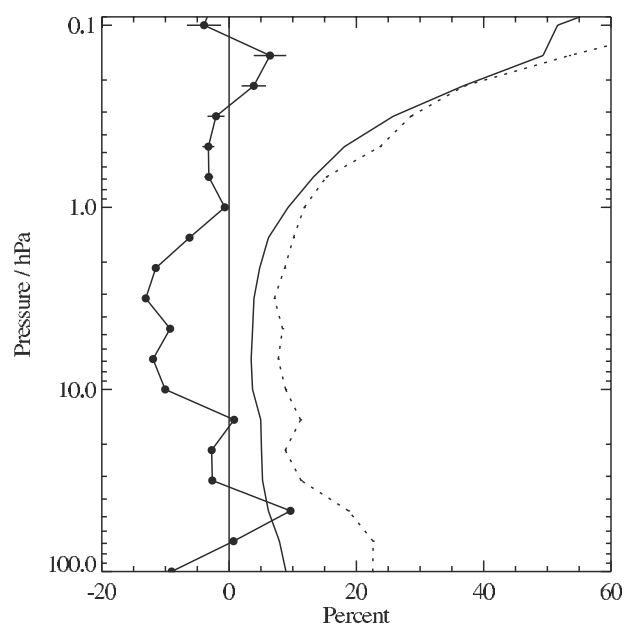


**Figure 15.** Similar to Figure 7 but for differences between MLS (v2.2) and MIPAS (Oxford University retrievals, see text), based on a fraction of one day's comparisons (for 373 profile coincidences) for 28 January 2005.

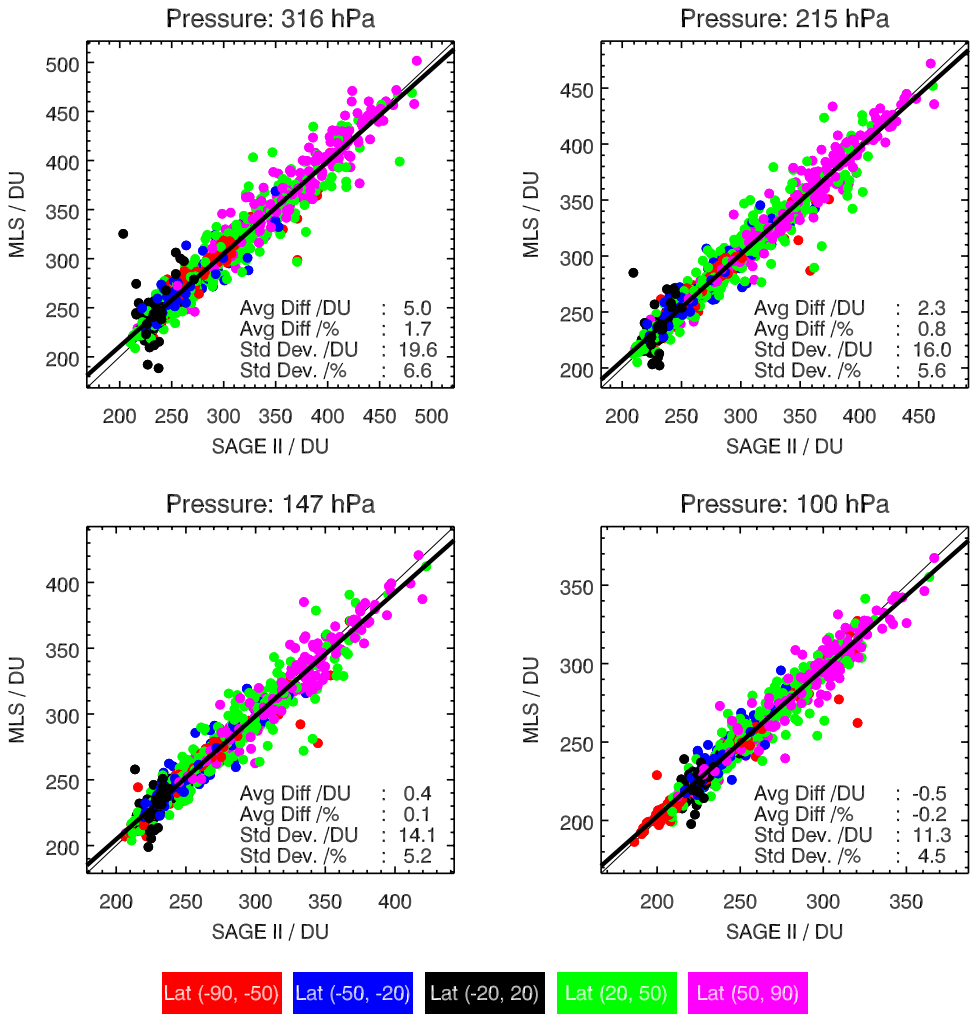


**Figure 16.** Comparison of MLS column ozone abundances (in Dobson units (DU)) versus columns obtained from integrated SAGE II ozone profiles between August 2004 and August 2005 and coincident with the MLS profiles (here within 1° latitude, 4° longitude); color coding for different latitude bins is indicated in the legend. The thick line is a linear fit to the data and the thin line shows unit slope. Average differences given above are for MLS − SAGE II.

arise from the MLS retrievals themselves, although an exact cause has not been identified.

### 3.1.5. MLS and MIPAS Profiles

[36] The Michelson Interferometer for Passive Atmospheric Sounding (MIPAS) [*Fischer and Oelhaf*, 1996] was launched on the European Space Agency (ESA) Environmental Satellite (Envisat) in March 2002 into a 98.5° inclination orbit. MIPAS is a Fourier Transform Spectrometer detecting limb emission in the infrared spectral region 685–2410 $cm^{-1}$ (4.1–14.6 $\mu$m) with a spectral resolution of 0.025 $cm^{-1}$. MIPAS operations were suspended in March 2004 because of an interferometer mechanism anomaly and restarted in January 2005 with a degraded spectral resolution of 0.0625$cm^{-1}$ and modified duty cycle and scan sequence to extend instrument lifetime [*Piccolo and Dudhia*, 2007]. MIPAS observes temperature, aerosols and a large number of minor constituents, including ozone. The horizontal along-track sampling interval of the MIPAS measurements taken in the nominal reduced-resolution mode is ~410 km, latitude coverage is 90°S to 90°N, and the vertical sampling is 1.5 to 4 km with a vertical range of 6 to 70 km. In addition to the ESA operational data products [*Raspollini et al.*, 2006], several institutions funded by the ENVISAT Calibration/Validation Program have developed off-line data processing capabilities for MIPAS. Here we show comparisons with off-line MIPAS ozone retrievals from algorithms developed at the University of Oxford (A. Dudhia and C. Waymark, personal communication, 2006). The MIPAS profiles were supplied with a cloud flag that has been used for data screening.

[37] In Figure 15, a single day of MIPAS retrievals is compared to the MLS $O_3$ data for that day. These results are in very good agreement, although in the midstratosphere the MIPAS values are larger than MLS by about 10%. This difference does not show the same characteristics as the upper stratospheric bias between MLS and ACE-FTS shown earlier, and we do not see such a bias versus SAGE II (Figure 7), HALOE (Figure 10), ground-based lidars [*Jiang et al.*, 2007], or ground-based microwave [e.g., *Boyd et al.*, 2007]. These limited comparisons show average

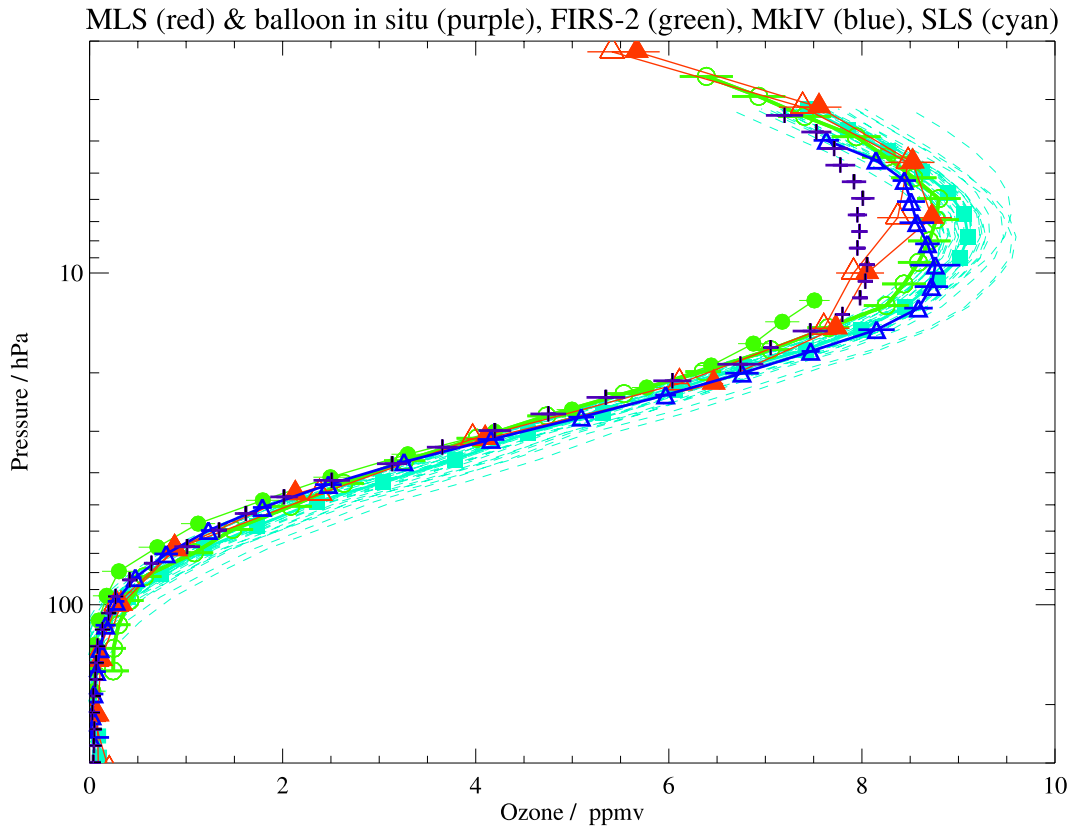


**Figure 17.** Balloon-borne ozone measurements from Ft. Sumner on 20 and 21 September 2005 in comparison to nearby MLS v2.2 ozone profiles, shown as open red triangles for daytime Aura overpass and closed red triangles for nighttime. Vertically averaged values from the fine-resolution UV photometer in situ measurements are shown as purple crosses, with variability within each altitude range given by horizontal error bars. FIRS-2 profiles closest in time to the daytime and nighttime overpasses are shown as open and closed green dots, respectively, with precision shown as error bars; the nighttime FIRS-2 profile retrieval is limited to heights below 29 km, where most profile information exists, as the nighttime balloon float altitude dropped below this level. MkIV retrievals (sunset) are shown as open blue triangles with error bars. SLS profiles (mainly for daytime) are depicted by the cyan dashed curves, with averages given by the cyan squares.

agreement within 10%, as well as good latitudinal correspondence (although not shown here) in both the stratosphere and lower mesosphere, with ozone increases into the polar night at high altitude (up to 0.05 hPa). However, more detailed comments about MIPAS and MLS differences or biases should await further work, as we are not aware of other related validation for this limited data set. However, the recent study by *Boyd et al.* [2007] provides comparisons of ground-based microwave data versus MIPAS operational ozone retrievals, as well as versus MLS ozone, for altitudes up to about 70 km; this work indicates that the MLS ozone retrievals are worth using for scientific studies into the upper mesosphere.

### 3.1.6. MLS Column Ozone Abundances

[38] *Yang et al.* [2007] show that the MLS v1.5 column ozone abundances calculated down to the tropopause give excellent agreement with SAGE II columns and are often a few DU larger than the SAGE II columns, for MLS columns down to 215 hPa in particular; they also report that SAGE III and HALOE ozone columns depart slightly more from MLS, but straddle both SAGE II and MLS values. The slight reduction in the MLS v2.2 columns brings SAGE II and MLS columns into even better agreement. *Petropavlovskikh et al.* [2008] find that MLS v2.2 ozone column abundances agree well with aircraft-based column data from the CAFS instrument on several Aura Validation Experiment (AVE) campaigns.

[39] Figure 16 shows a comparison between MLS and SAGE II column ozone for coincident profiles using available v2.2 MLS data and SAGE II profiles from August 2004 to August 2005. Average column results from SAGE II and MLS are in very good agreement (within 1%) down to 215 hPa; standard deviations of the differences are about 5%, and reach 16 DU at 215 hPa. It would be good to have an even better characterization of column ozone for the calculation of residual columns using MLS and OMI data, although the scatter is consistent with about 2% precision arising from MLS, a similar contribution from SAGE II, as well as an atmospheric variability component arising from imperfect coincidences. *Jiang et al.* [2007] have compared

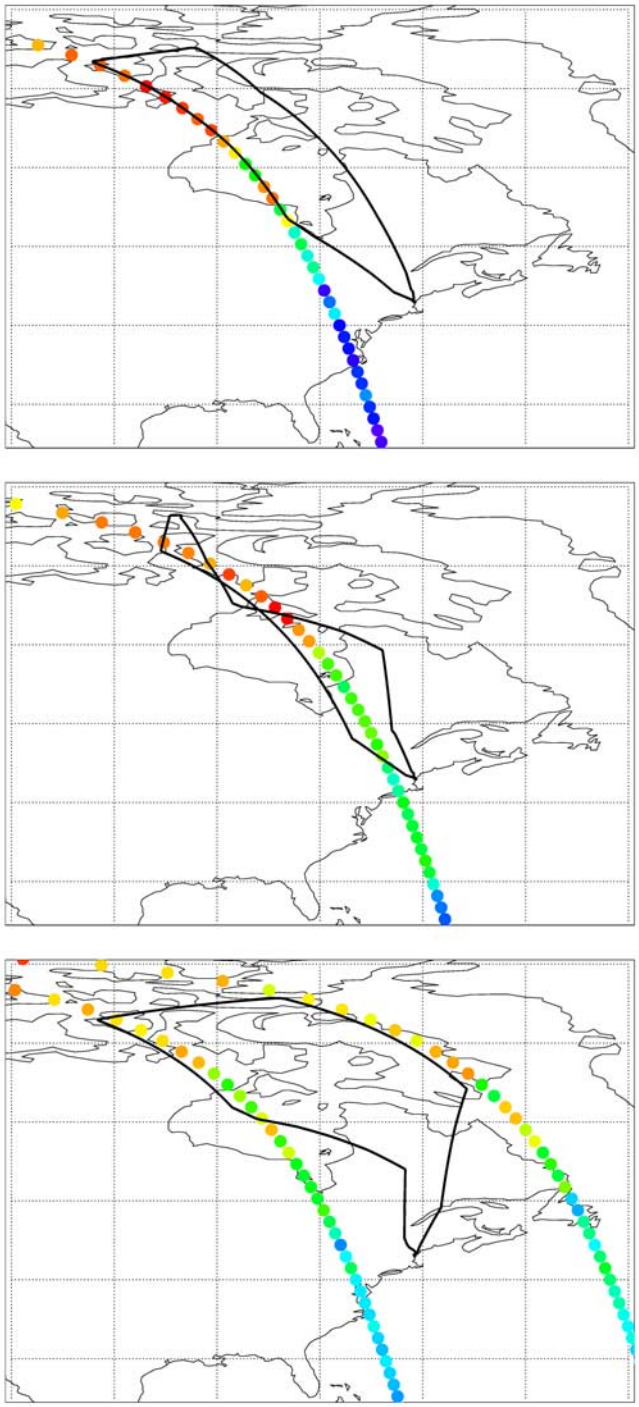

**Figure 18.** Maps depicting the PAVE campaign DC-8 aircraft tracks (solid thick black lines) during 3 d (for (top) 27 January, (middle) 31 January, and (bottom) 5 February 2005) and superimposed MLS profile locations for coincident satellite suborbital tracks shown by colored dots. The dots' color scheme (not shown) corresponds to ozone values at 100 hPa; a more quantitative measure of the compared ozone data from various altitudes is provided in Figures 19–21. Figure 18 (bottom) results are considered from two close-coincidence legs: the first leg on the outbound, eastern side and the second leg on the inbound, western side.

MLS and ozonesonde partial column abundances, and find somewhat poorer results than for MLS and SAGE II shown here. This may be because the MLS columns for the SAGE II comparisons extend to higher altitudes than typical sonde data, and MLS ozone is biased slightly lower than SAGE II ozone in that region.

### 3.2. Comparisons With Balloon Data

[40] Comparisons between MLS v1.5 data and measurements from balloons launched from Ft. Sumner, New Mexico, in September 2004 have been discussed by *Froidevaux et al.* [2006a]. Small changes in MLS v2.2 ozone do not alter the main conclusions; for example, there is typically better than ~5% agreement between MLS v2.2 ozone from 100 to 10 hPa and the 2004 data from the in situ UV photometer, whose accuracy is estimated to be <5%. Another large balloon campaign was carried out from Ft. Sumner in September 2005; see *Froidevaux et al.* [2006a] for a brief description of the balloon-borne instruments, excluding the JPL Submillimeterwave Limb Sounder 2 (SLS-2). This new instrument includes cooled components and provides much greater sensitivity than an earlier SLS version; SLS-2 measures ozone and various other trace gases from scans of the limb thermal emission near 600 GHz. A vertical resolution of 2 to 3 km is achieved by SLS-2 and the other remote sensing balloon instruments, the JPL MkIV Fourier Transform Infrared (FTIR) spectrometer, performing solar occultation observations in the 650 to 5650 $cm^{-1}$ region at 0.01 $cm^{-1}$ spectral resolution [*Toon*, 1991], and the Smithsonian Astrophysical Observatory (SAO) far infrared spectrometer 2 (FIRS-2), measuring thermal emission at 6–120 $\mu$m with a spectral resolution of 0.004 $cm^{-1}$ [*Johnson et al.*, 1995]. Figure 17 displays the balloon ozone data, in comparison to the closest daytime and nighttime MLS profiles; the MLS profiles fall in the midst of the balloon data, which differ among themselves by more than 5% in places. The change in slope near 15 hPa in the in situ profile is captured by the MLS retrievals, although MLS values are 5 to 9% larger near the peak, as are most of the other balloon profiles, possibly because of atmospheric inhomogeneities. On average, the MLS results between 215 and 3 hPa are 4% larger than the in situ photometer data, with a standard deviation of 7%. The MkIV profile peak occurs below the peaks in the profiles from MLS, FIRS-2, and SLS, possibly because the MkIV measurements sample a different atmospheric region than the emission instruments. These results confirm the validity of MLS ozone, although not enough statistics have been provided by large balloons to remove most of the random error components in such comparisons and identify biases that could exceed the MLS stratospheric accuracy estimates of 5 to 7%.

### 3.3. Comparisons With Aircraft Data

[41] One of the high priority requests for validation data from campaigns in support of the Aura measurements of ozone profiles, as part of the prelaunch planning for Aura validation [*Froidevaux and Douglass*, 2001], was aircraft lidar measurements along the suborbital MLS track, in order to compare "curtain plots" retrieved from the lidar and satellite instruments. A series of such comparisons was enabled in a powerful way during the Polar Aura Validation

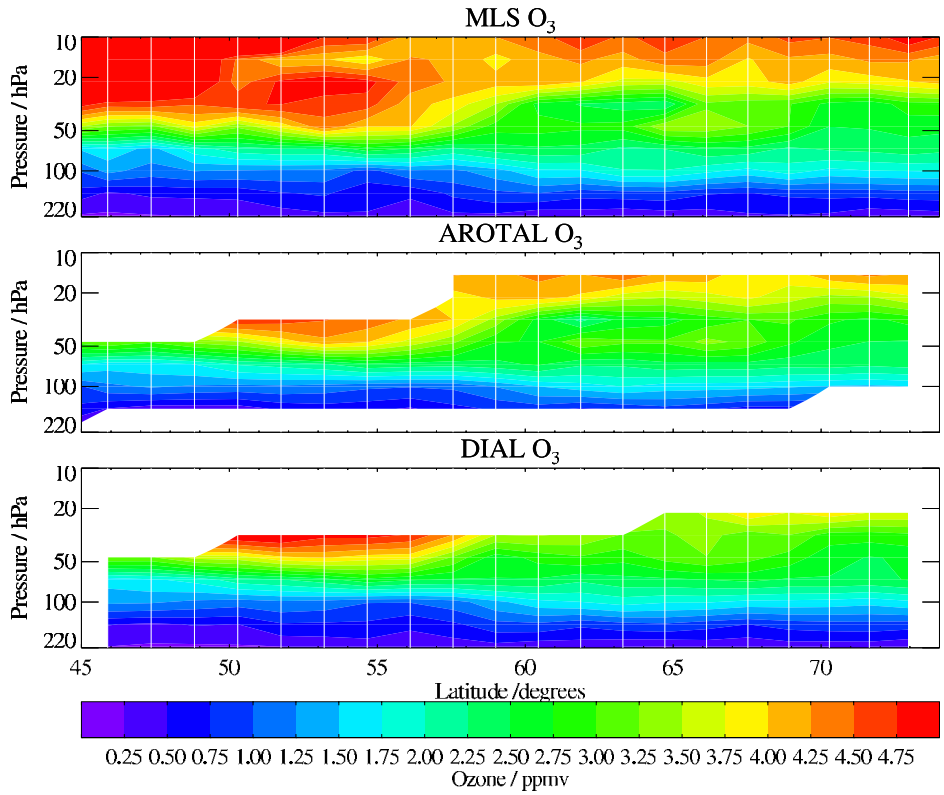


**Figure 19.** Lidar and MLS ozone curtain plots for 31 January 2005 during the PAVE campaign. (top) MLS, (middle) AROTAL, and (bottom) DIAL retrievals are provided with the lidar data smoothed to the vertical and horizontal spacing appropriate for MLS (with profile locations indicated by white vertical lines), as discussed in the text.

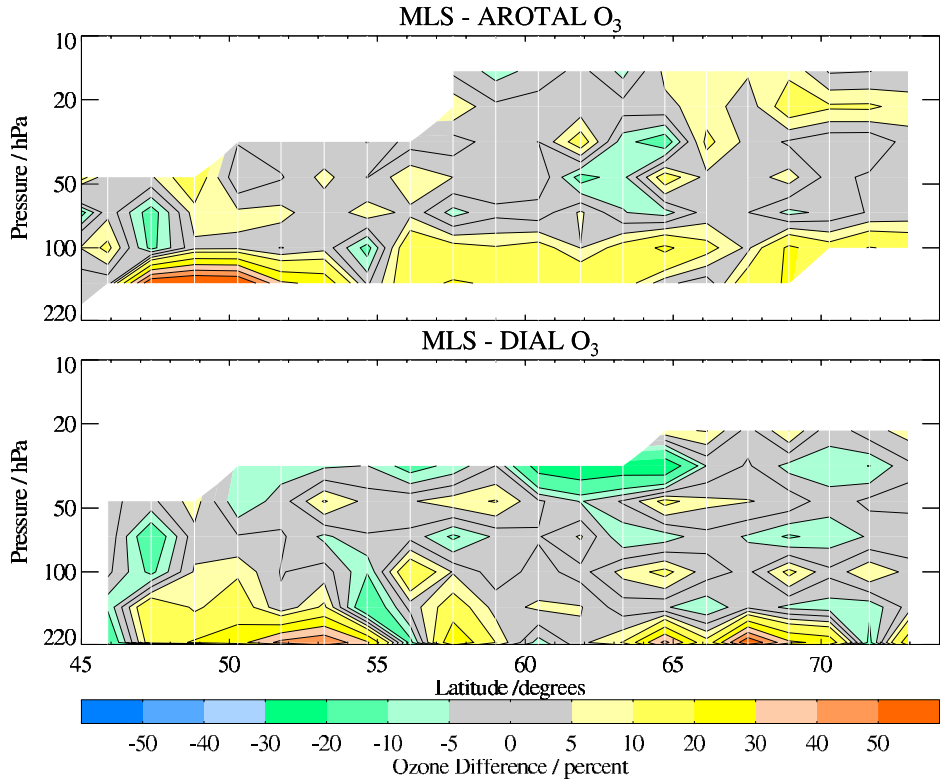


**Figure 20.** Percent differences for MLS ozone minus lidar ozone retrievals, corresponding to the abundances shown in Figure 19.

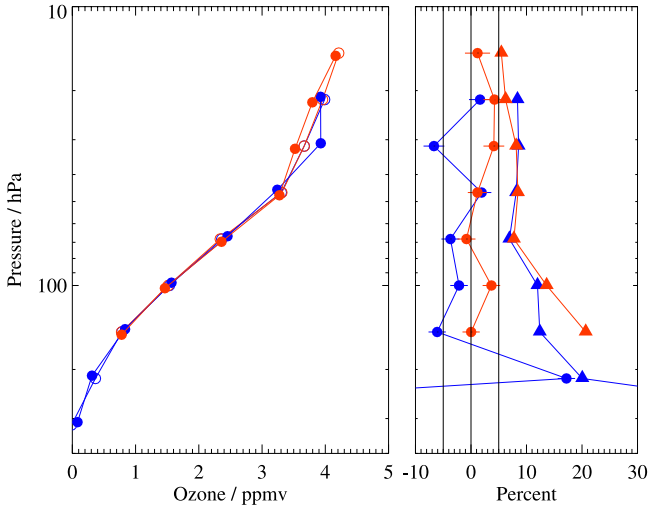


**Figure 21.** Summary of the average MLS and aircraft lidar ozone profiles for the combined set (see text) of coincident DC-8 and MLS measurements during 3 d of the PAVE 2005 campaign, as illustrated in Figure 18. (left) Average ozone abundances from DIAL (solid blue circles) on the MLS vertical retrieval grid (see text) and from AROTAL (solid red circles) are compared to averages from MLS (open circles, with red and blue values very close to each other for the averages corresponding to good DIAL and AROTAL data). (right) The corresponding percent ozone differences are shown for MLS minus DIAL (solid blue circles) and MLS minus AROTAL (solid red circles), with the standard deviation of the differences shown as triangles of the corresponding colors. Error bars on the average differences represent twice the precision (standard error) in the mean differences. Values at 316 hPa are shown on Figure 21 (left) but not as percent differences (off scale); this level is not generally recommended for MLS ozone data usage.

Experiment (PAVE), a campaign in January/February 2005, during which the NASA DC-8 conducted several flights into the Arctic polar vortex. Both the airborne Differential Absorption Lidar (DIAL) and the Airborne Raman Ozone, Temperature, and Aerosol Lidar (AROTAL) instruments were onboard the DC-8 during the flights, portions of which were often planned to coincide with the MLS suborbital track. Airborne lidar measurements from DIAL and AROTAL have a long history [e.g., *Browell et al.*, 1990, 1998, 2003; *McGee et al.*, 1995; *Lait et al.*, 2004]. *Schoeberl et al.* [2006b] illustrate some of the atmospheric features, including polar vortex filamentation, observed by both the aircraft and Aura MLS during the PAVE campaign. AROTAL uses Rayleigh scattered signals from a pair of lasers transmitting at 308 and 355 nm to measure ozone, temperature, and aerosols. Lidar data are acquired in 15 m bins, read out every 20 s, and integrated for several minutes, to provide a running mean ozone profile every 20s. The vertical resolution varies between 0.75 and 3 km. The DIAL instrument utilizes two lasers (using 301 and 310 nm wavelengths) and provides ozone data at (typically) 0.5 to 0.7 km vertical resolution above and below the aircraft, with a roughly 0.75 km gap just above and below the aircraft altitude; this gap has been filled in by interpolation, using in situ data from the Fast Response Ozone (FASTOZ) measurements aboard the aircraft [see also *Browell et al.*, 2003]. The archived DIAL data are provided roughly every minute of flight time (or about 14 km horizontal distance), based on 5-min running averages. Lidar ozone mixing ratios are calculated from number densities (the original lidar retrievals) and the Goddard Space Flight Center (GSFC) Assimilation gridded atmospheric density profiles interpolated along the aircraft flight track (kindly provided by GSFC codes 610.1 and 613.3). Flights were timed to have the Aura overpass occur within the flights' temporal extent, which lasted a number of hours as opposed to the minute or two Aura overpass time.

[42] Figure 18 shows a map with the aircraft tracks north of Portsmouth, New Hampshire (the DC-8 base for this campaign), along with superimposed MLS profile locations for the flights of 27 January, 31 January, and 5 February 2005. These 3 d provide the best coincident measurements from the lidars and MLS; the two legs of close coincidence with the two MLS daytime tracks on 5 February are spaced by about 1 h and a half. Figure 19, for 31 January, provides a striking example of one of the accomplishments of this aircraft validation campaign, as it shows the very similar ozone distributions obtained from the (near coincident) MLS and lidar measurements in this region of strong latitudinal gradients. The lidar data have been smoothed using a two-dimensional least squares routine to compare on the same grid (horizontal and vertical) as the MLS profiles. Figure 20 gives the cross section of percent differences (MLS minus lidar) for 31 January; the MLS and lidar values are often within 5%, with somewhat larger differences in the 150 to 215 hPa range. Similar percent differences are obtained on other flights. Figure 21 provides a summary of the average profiles for all 4 flight legs shown in Figure 18; occasional bad lidar data can produce slight differences in the MLS averages that are appropriate for the two lidar data sets. AROTAL lidar measurements can be used at somewhat higher altitudes than DIAL, and the DIAL data, coupled with FASTOZ measurements are used for the higher pressures (at and below the aircraft). Percent differences between MLS and DIAL or AROTAL profiles, as well as standard deviations of the differences are shown in Figure 21 (right); the error bars on these points indicate twice the precision (standard error) in the mean differences, based on the MLS precision values and a value of 5% precision to account for the lidar uncertainty, including the translation of ozone abundances to mixing ratios versus pressure via the meteorological "curtain files" provided by GSFC. There are enough statistics here to make differences stand out above the random uncertainties. The MLS averages between 20 and 150 hPa are very close to (within 6% of) both AROTAL and DIAL measurements. These differences are within the combined accuracies of the MLS and lidar data. The MLS high bias at 215 hPa is not as clearly evident in comparisons of MLS with the downward-looking DIAL during the Spring of 2006 Intercontinental Chemical Transport Experiment B (INTEX-B) campaign [*Livesey et al.*, 2008].

[43] Figure 22 shows curtain plots and percent differences versus AROTAL data gathered during the INTEX-B DC-8 nighttime transit flight from Hawaii to Anchorage, Alaska, on 1 May 2006. Portions of the lidar data file with

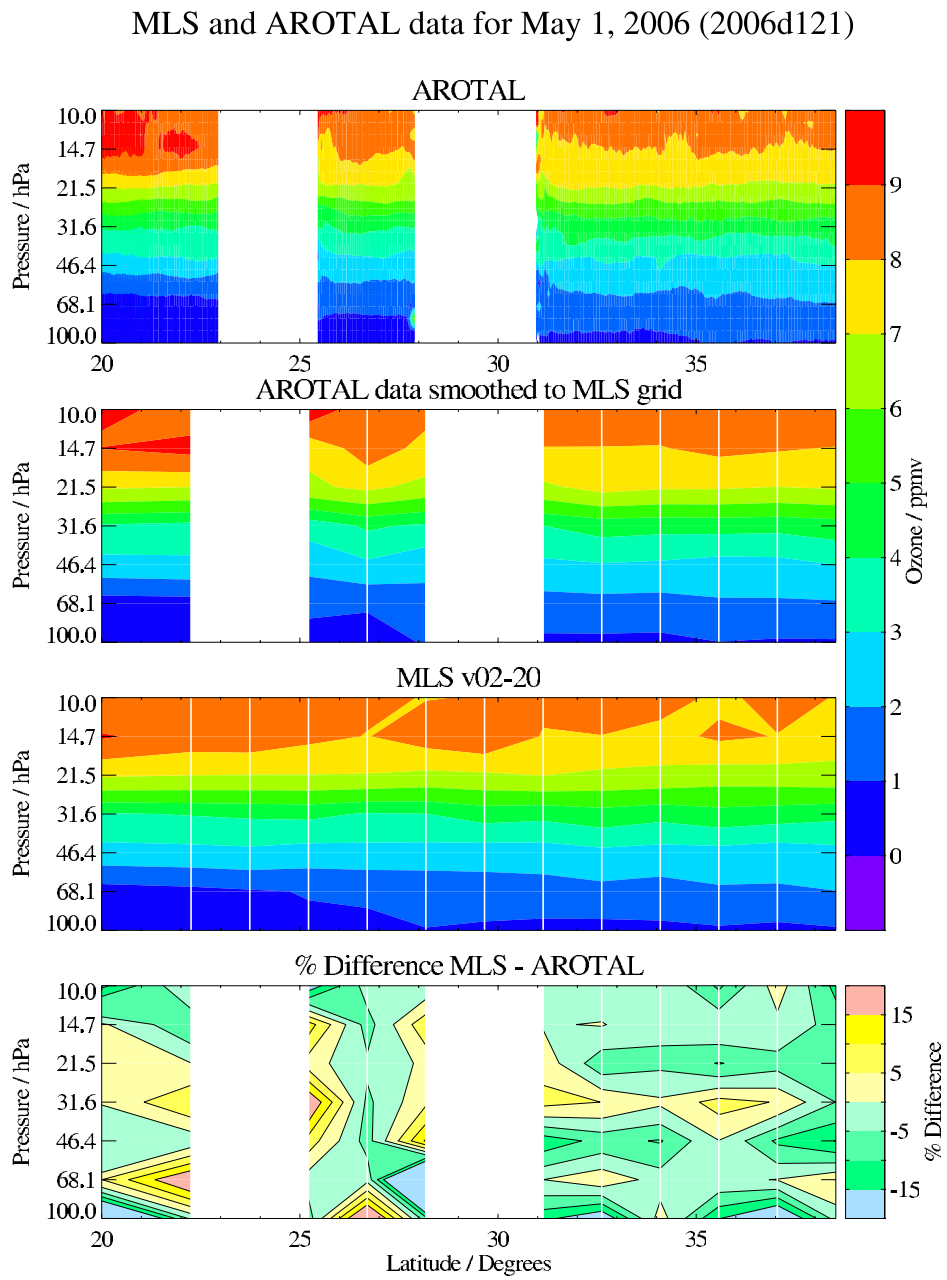


**Figure 22.** INTEX-B lidar ozone data from AROTAL on 1 May 2006, obtained during the DC-8 transit flight from Hawaii to Alaska, are compared to MLS nighttime profiles at nearby locations. (top) The lidar curtain plot at fine resolution, (top middle) the lidar data degraded to the MLS vertical and horizontal grid (see text), (bottom middle) the MLS ozone abundances, and (bottom) the percent difference (MLS – AROTAL).

no data (or bad data) for this flight may be causing a few undesirable effects during the smoothing process for these comparisons, and the flight track was more removed (by up to a few degrees for the latitudes shown here) from the MLS track than during the PAVE flights. However, the MLS/lidar differences from 100 to 10 hPa are about 5 to 10% for this flight, with standard deviations of 5% (near 20 hPa) to 18% (at 100 hPa). Both instruments observe very similar gradients from the tropical latitudes to midlatitudes, notably in the lower stratosphere. Another nighttime flight (also targeted more at the HIRDLS track) occurred on 22 March 2006, during transit from Houston to NASA Ames. Again, excellent agreement is obtained (see Figure 23): average differences are within 6% for 7 to 46 hPa, and 10% at 68 hPa, with standard deviations from 4% to 12% at all heights. On average, these two nighttime flights give differences between MLS and AROTAL that are within 2% from 10 hPa to 46 hPa, and 6% and 10% (MLS slightly lower than AROTAL) for 68 and 100 hPa, respectively. A daytime DC-8 flight coincidence with the MLS track (from about 34°N to 44°N) on 25 April 2006 gives slightly larger (10–15%) differences between MLS and AROTAL over a

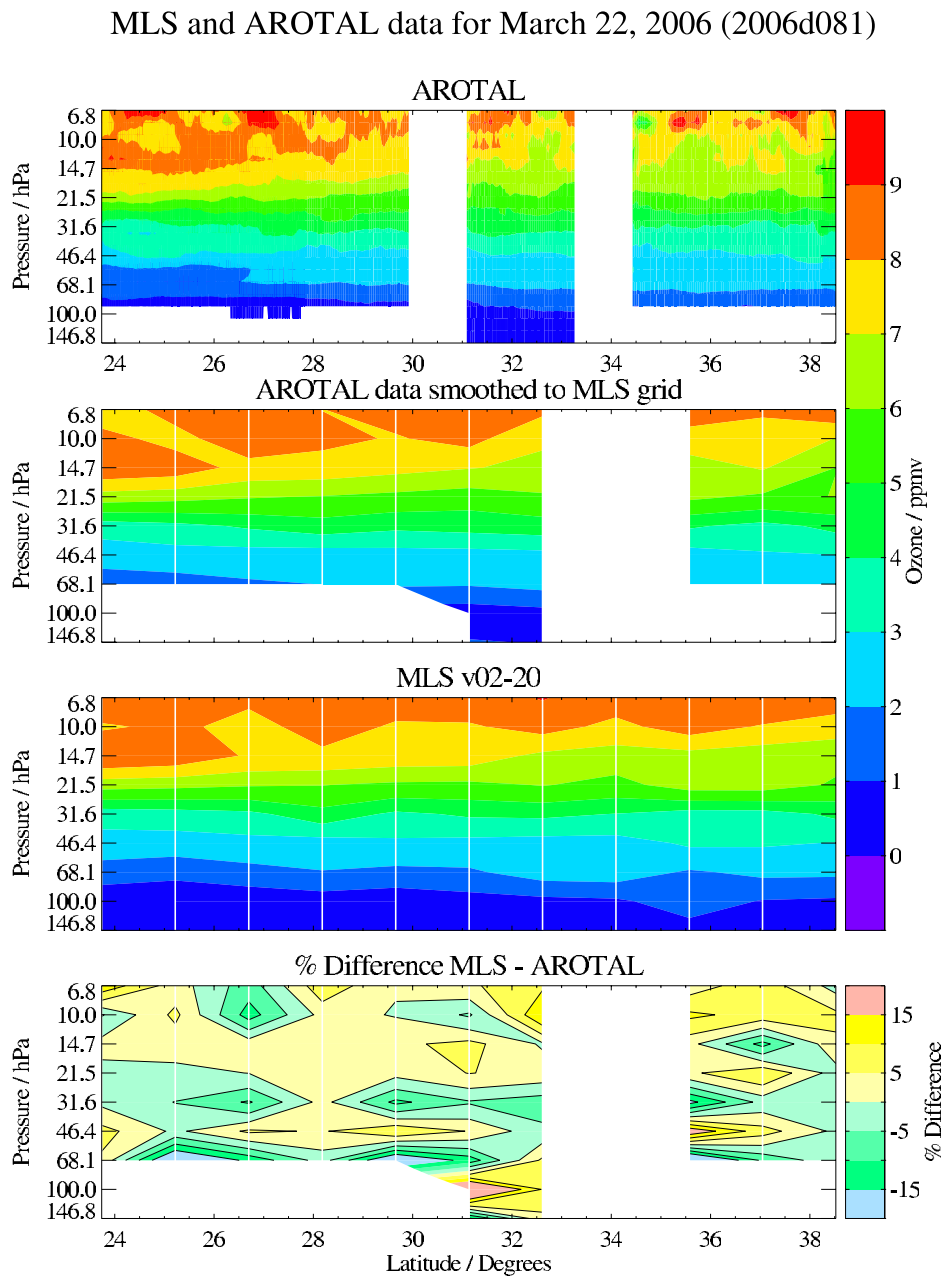


**Figure 23.** Same as Figure 22 but for MLS comparison with INTEX-B AROTAL ozone lidar profiles obtained on 22 March 2006, during the DC-8 transit flight from Houston to NASA Ames.

narrower available vertical range (details not shown here), probably because of difficulties in obtaining optimum lidar background calibration under large solar flux conditions (high sun).

[44] Overall, the combination of lidar and MLS ozone data during such aircraft campaigns successfully demonstrates that the satellite and aircraft measurements offer a similar view of the atmosphere, despite their vastly different raw measurement characteristics.

## 4. Summary and Conclusions

[45] Table 2 gives a summary of the estimated resolution, precision, and accuracy of MLS v2.2 ozone. Some of the results given in Table 2 overlap with the results regarding MLS ozone at the highest pressures (upper troposphere), which are the focus of the analyses by *Livesey et al.* [2008]. The accuracy for 215 hPa has been increased from its theoretical estimate of 20 ppbv + 10% to 20 ppbv + 20%, based mainly on the results of MLS comparisons versus ozonesondes [*Jiang et al.*, 2007].

[46] MLS data users should follow the data screening criteria discussed in this paper (section 2.3), as there have been some changes from version 1.5. The MLS standard ozone product from the v2.2 retrievals is in very good agreement with other well established data sets. Over much of the stratosphere (from 1 to 100 hPa), the estimated accuracy of MLS ozone is about 8% or better, based on sensitivity estimates using different options for input parameters to the MLS retrievals, and consistent with comparisons

**Table 2.** Summary of MLS v2.2 Ozone Characteristics at Selected Pressure Levels

| Pressure, hPa | Resolution (Vertical × Horizontal),[a] km | Precision[b] Parts per Million by Volume | Precision[b] Percent | Accuracy[c] Parts per Million by Volume | Accuracy[c] Percent | Comments |
|---|---|---|---|---|---|---|
| ≤0.01 | — | — | — | — | — | Not generally recommended for scientific use (but some information exists in averages). |
| 0.02 | 6 × 200 | 1.0 | 200 | 0.1 | 35 | |
| 0.05 | 6 × 200 | 0.6 | 100 | 0.2 | 30 | |
| 0.1 | 4 × 300 | 0.4 | 40 | 0.2 | 20 | |
| 0.2 | 3 × 300 | 0.4 | 30 | 0.1 | 7 | |
| 0.5 | 3 × 300 | 0.3 | 15 | 0.1 | 5 | |
| 1 | 3 × 250 | 0.3 | 10 | 0.2 | 7 | |
| 2 | 3 × 250 | 0.2 | 5 | 0.2 | 5 | |
| 5 | 3 × 200 | 0.2 | 3 | 0.3 | 5 | |
| 10 | 3 × 200 | 0.2 | 3 | 0.3 | 5 | |
| 22 | 3 × 200 | 0.1 | 2 | 0.2 | 5 | |
| 46 | 3 × 200 | 0.1 | 4 | 0.2 | 8 | |
| 68 | 3 × 200 | 0.05 | 3–10 | 0.05 | 3–10 | |
| 100 | 3 × 200 | 0.04 | 2–30 | 0.05 + 5% | — | |
| 150 | 3 × 200 | 0.04 | 5–100 | 0.02 + 5% | — | |
| 215 | 3 × 200 | 0.04 | 5–100 | 0.02 + 20% | — | |
| >300 | — | — | — | — | — | Not recommended for scientific use (not retrieved for pressures >316 hPa). |

[a]Horizontal resolution is in the along-track direction, and the (along-track) separation between adjacent retrieved profiles is 1.5° great circle angle (∼165 km); cross-track resolution is ∼6 km.
[b]Precision is 1$\sigma$ estimate for individual profiles.
[c]Systematic uncertainty, 2$\sigma$ estimate of probable magnitude (see text).

to well established satellite ozone data sets and to ozonesondes [see *Jiang et al.*, 2007]. For example, comparisons of MLS versus SAGE II ozone show agreement within a few to 7% for the stratosphere, and as low down as 147 hPa. Some high MLS biases (∼20% globally) are apparent at 215 hPa (the bottom recommended level for MLS), in comparisons versus ozonesondes [*Jiang et al.*, 2007]. A systematic MLS bias at 215 hPa of about 10–20% is also indicated by MLS comparisons with SAGE II and PAVE lidar data, although this is not discerned from MLS and aircraft in situ and DIAL lidar ozone comparisons during the INTEX-B campaign [*Livesey et al.*, 2008].

[47] The average differences between MLS and other satellite ozone retrievals in the lower stratosphere often exhibit oscillations of a few percent in amplitude (e.g., with a positive notch at 22 hPa); while the MLS retrievals appear to generally be the source of such oscillations, the impact on most scientific investigations should be minimal.

[48] Other recent analyses of MLS and solar occultation data (including SAGE III) by *Manney et al.* [2007] support the statements made here regarding the quality of the MLS standard ozone product. Furthermore, excellent agreement (mostly within ∼5%) is obtained in comparisons between MLS and ground-based microwave data into the mesosphere [*Hocke et al.*, 2007; *Boyd et al.*, 2007]. There are well-known comparison and retrieval difficulties when large line of sight gradients exist along the measurement raypaths, such as for mesospheric $O_3$ retrievals from solar occultation. Further careful mesospheric ozone comparisons between MLS and MIPAS, or using mesospheric measurements from the Sounding of the Atmosphere with Broadband Emission Radiometry (SABER) or the Global Ozone Monitoring by Occultation of Stars (GOMOS) experiments could prove useful in expanding mesospheric validation efforts.

[49] The MLS stratospheric column ozone abundances have been shown to be in excellent agreement with SAGE II column ozone data, which confirms the results of *Ziemke et al.* [2006] and *Yang et al.* [2007], who used mostly v1.5 MLS data. MLS column abundances have also been shown to be in good agreement (within a few percent) with aircraft measurements [*Petropavlovskikh et al.*, 2008], and ozonesonde partial columns [*Jiang et al.*, 2007], although a high MLS bias is evident in some of the comparisons (mostly in the tropics) from the latter reference. *Schoeberl et al.* [2007] also discuss a possible high MLS bias in their analyses of MLS v1.5 column data. The stratospheric MLS columns have been reduced in v2.2 (by 0.5 to 2%), in comparison to v1.5, mitigating but maybe not eliminating such column biases.

[50] The latitudinal distributions obtained by satellite (coincident) profiles and the aircraft-based lidar "curtains" along the suborbital MLS track show very good agreement with MLS distributions, with a few small offsets. Results of detailed temporal comparisons await more studies with additional version 2.2 MLS data, but 5% agreement with other satellite data sets must imply that there is overall good tracking of seasonal changes, for example. Good agreement in ozone temporal variations from 2004 to 2006 between MLS (v1.5) data and sample data from ozonesonde and lidar (at northern midlatitudes) is illustrated by *Jiang et al.* [2007]. We also observe that the v2.2 MLS data track the v1.5 data very well as a function of time. Information about stratospheric variations on timescales of the quasi-biennial oscillation (QBO) is now also emerging from the Aura MLS data set [*Schoeberl et al.*, 2008]. Finally, the MLS ozone measurements have been shown to significantly improve data assimilation results [*Feng et al.*, 2008; *Jackson*, 2007; *Stajner et al.*, 2008].

[51] We expect that much more knowledge will be forthcoming in years to come, based on MLS and Aura ozone data in general, regarding stratospheric and tropospheric ozone variations, with connections to the issue of air quality from regional to global scales, as well as to climate change.

[52] **Acknowledgments.** This work at the Jet Propulsion Laboratory, California Institute of Technology, was performed under contract with the National Aeronautics and Space Administration. We are very grateful to the MLS instrument and data/computer operations and development team (at JPL and from Raytheon, Pasadena) for their support through all the phases of the MLS project, in particular D. Flower, G. Lau, J. Holden, R. Lay, M. Loo, G. Melgar, D. Miller, B. Mills, M. Echeverri, E. Greene, A. Hanzel, A. Mousessian, S. Neely, C. Vuu, and P. Zimdars. We greatly appreciate the efforts of B. Bojkov and the Aura Validation Data Center (AVDC) team, whose work facilitated the MLS validation activities. We thank A. Dudhia and C. Waymark at Oxford University for their role in providing MIPAS ozone retrievals discussed in this work, and we thank I. Boyd and A. Parrish for comments on day and night mesospheric ozone comparisons. We also acknowledge the work of the satellite instrument and science teams from SAGE II, HALOE, and POAM III, who provided readily available high-quality data that helped us provide timely validation analyses for the MLS retrievals. Thanks to the Aura Project for their support throughout the years (before and after the Aura launch), in particular M. Schoeberl, A. Douglass (also as cochair of the Aura validation working group), E. Hilsenrath, and J. Joiner. We also acknowledge the support from NASA Headquarters; P. DeCola for MLS and Aura; and M. Kurylo, J. Gleason, B. Doddridge, and H. Maring, especially in relation to the Aura validation activities and campaign planning efforts. The aircraft campaigns themselves involved tireless hours of planning from various coordinators, including E. Jensen, M. Schoeberl, H. Singh, D. Jacob, and others, as well as K. Thompson and others involved with campaign flight management and support. We express our thanks to the DIAL, AROTAL, and FASTOZ instrument and data analysis teams for their efforts in association with the PAVE field experiment, and we express our thanks to the Columbia Scientific Balloon Facility for launching the balloon experiments whose data are used in this work. Funding for ACE was provided by the Canadian Space Agency and the Natural Sciences and Engineering Research Council (NSERC) of Canada.

## References

Barret, B., et al. (2006), Intercomparisons of trace gases profiles from the Odin/SMR and Aura/MLS limb sounders, *J. Geophys. Res.*, *111*, D21302, doi:10.1029/2006JD007305.

Bernath, P. F., et al. (2005), Atmospheric Chemistry Experiment (ACE): Mission overview, *Geophys. Res. Lett.*, *32*, L15S01, doi:10.1029/2005GL022386.

Bhatt, P. P., E. E. Remsberg, L. L. Gordley, J. M. McInerney, V. G. Brackett, and J. M. Russell III (1999), An evaluation of the quality of Halogen Occultation Experiment ozone profiles in the lower stratosphere, *J. Geophys. Res.*, *104*, 9261–9275, doi:10.1029/1999JD900058.

Boone, C. D., et al. (2005), Retrievals for the Atmospheric Chemistry Experiment Fourier-Transform Spectrometer, *Appl. Opt.*, *44*, 7218–7231, doi:10.1364/AO.44.007218.

Borchi, F., J.-P. Pommereau, A. Garnier, and M. Pinharanda (2005), Evaluation of SHADOZ sondes, HALOE and SAGE II ozone profiles at the tropics from SAOZ UV-Vis remote measurements onboard long duration balloons, *Atmos. Chem. Phys.*, *5*, 1381–1397.

Boyd, I. S., A. D. Parrish, L. Froidevaux, T. von Clarmann, E. Kyrölä, J. M. Russell III, and J. M. Zawodny (2007), Ground-based microwave ozone radiometer measurements compared with Aura-MLS v2.2 and other instruments at two Network for Detection of Atmospheric Composition Change sites, *J. Geophys. Res.*, *112*, D24S33, doi:10.1029/2007JD008720.

Browell, E. V., et al. (1990), Airborne lidar observations in the wintertime Arctic stratosphere: Ozone, *Geophys. Res. Lett.*, *17*, 325–328, doi:10.1029/GL017i004p00325.

Browell, E. V., S. Ismail, and W. B. Grant (1998), Differential Absorption Lidar (DIAL) measurements from air and space, *Appl. Phys. B*, *67*, 399–410, doi:10.1007/s003400050523.

Browell, E. V., et al. (2003), Large-scale ozone and aerosol distributions, air mass characteristics, and ozone fluxes over the western Pacific Ocean in late winter/early spring, *J. Geophys. Res.*, *108*(D20), 8805, doi:10.1029/2002JD003290.

Feng, L., R. Brugge, E. V. Holm, R. S. Harwood, A. O'Neill, M. J. Filipiak, L. Froidevaux, and N. J. Livesey (2008), Four-dimentional variational assimilation of ozone profiles from the Microwave Limb Sounder on the Aura satellite, *J. Geophys. Res.*, doi:10.1029/2007JD009121, in press.

Fischer, H., and H. Oelhaf (1996), Remote sensing of vertical profiles of atmospheric trace constituents with MIPAS limb-emission spectrometers, *Appl. Opt.*, *35*, 2787–2796.

Froidevaux, L., and A. Douglass (Eds.) (2001), Earth Observing System (EOS) Aura science data validation plan, version 1.0, report, Goddard Space Flight Cent., Greenbelt, Md.

Froidevaux, L., et al. (1996), Validation of UARS Microwave Limb Sounder ozone measurements, *J. Geophys. Res.*, *101*, 10,017–10,060, doi:10.1029/95JD02325.

Froidevaux, L., et al. (2006a), Early validation analyses of atmospheric profiles from EOS MLS on the Aura satellite, *IEEE Trans. Geosci. Remote Sens.*, *44*(5), 1106–1121, doi:10.1109/TGRS.2006.864366.

Froidevaux, L., et al. (2006b), Temporal decrease in upper atmospheric chlorine, *Geophys. Res. Lett.*, *33*, L23812, doi:10.1029/2006GL027600.

Hocke, K., et al. (2007), Comparison and synergy of stratospheric ozone measurements by satellite limb sounders and the ground-based microwave radiometer SOMORA, *Atmos. Chem. Phys.*, *7*, 4117–4131.

Jackson, D. R. (2007), Assimilation of EOS MLS ozone observations in the Met Office data assimilation system, *Q. J. R. Meteorol. Soc.*, *133*, 1771–1788.

Jarnot, R. F., V. S. Perun, and M. J. Schwartz (2006), Radiometric and spectral performance and calibration of the GHz bands of EOS MLS, *IEEE Trans. Geosci. Remote Sens.*, *44*, 1131–1143, doi:10.1109/TGRS.2005.863714.

Jiang, Y. B., et al. (2007), Validation of Aura Microwave Limb Sounder Ozone by ozonesonde and lidar measurements, *J. Geophys. Res.*, *112*, D24S34, doi:10.1029/2007JD008776.

Johnson, D. G., K. W. Jucks, W. A. Traub, and K. V. Chance (1995), Smithsonian stratospheric far-infrared spectrometer and data reduction system, *J. Geophys. Res.*, *100*, 3091–3106.

Lait, L. R., et al. (2004), Non-coincident inter-instrument comparisons of ozone measurements using quasi-conservative coordinates, *Atmos. Chem. Phys.*, *4*, 2345–2352.

Livesey, N. J., et al. (2005), Version 1.5 level 2 data quality and description document, *Tech. Rep. JPL D-32381*, Jet Propul. Lab., Pasadena, Calif.

Livesey, N. J., et al. (2006), Retrieval algorithms for the EOS Microwave Limb Sounder (MLS), *IEEE Trans. Geosci. Remote Sens.*, *44*(5), 1144–1155, doi:10.1109/TGRS.2006.872327.

Livesey, N. J., et al. (2008), Validation of Aura Microwave Limb Sounder $O_3$ and CO observations in the upper troposphere and lower stratosphere, *J. Geophys. Res.*, *113*, D15S02, doi:10.1029/2007JD008805.

Lumpe, J. D., et al. (2003), Comparison of POAM III ozone measurements with correlative aircraft and balloon data during SOLVE, *J. Geophys. Res.*, *108*(D5), 8316, doi:10.1029/2001JD000472.

Manney, G. L., et al. (2007), Solar occultation satellite data and derived meteorological products: Sampling issue and comparisons with Aura Microwave Limb Sounder, *J. Geophys. Res.*, *112*, D24S50, doi:10.1029/2007JD008709.

McGee, T. J., M. Gross, U. N. Singh, J. J. Butler, and P. Kimvilankani (1995), An improved stratospheric ozone lidar, *Opt. Eng.*, *20*, 955–958.

Natarajan, M., L. E. Deaver, E. Thompson, and B. Magill (2005), Impact of twilight gradients on the retrieval of mesospheric ozone from HALOE, *J. Geophys. Res.*, *110*, D13305, doi:10.1029/2004JD005719.

Nazaryan, H., M. P. McCormick, and J. M. Russell III (2005), New studies of SAGE II and HALOE ozone profile and long-term change comparisons, *J. Geophys. Res.*, *110*, D09305, doi:10.1029/2004JD005425.

Petropavlovskikh, I., L. Froidevaux, R. Shetter, S. Hall, K. Ullmann, and P. K. Bhartia (2008), In-flight validation of Aura MLS ozone with CAFS partial ozone columns, *J. Geophys. Res.*, doi:10.1029/2007JD008690, in press.

Piccolo, C., and A. Dudhia (2007), Precision validation of MIPAS-Envisat products, *Atmos. Chem. Phys. Discuss.*, *7*, 911–929.

Randall, C. E., et al. (2003), Validation of POAM III ozone: Comparisons with ozonesonde and satellite data, *J. Geophys. Res.*, *108*(D12), 4367, doi:10.1029/2002JD002944.

Raspollini, P., et al. (2006), MIPAS level 2 operational analysis, *Atmos. Chem. Phys.*, *6*, 5605–5630.

Read, W. G., Z. Shippony, M. J. Schwartz, N. J. Livesey, and W. V. Snyder (2006), The clear-sky unpolarized forward model for the EOS Microwave Limb Sounder (MLS), *IEEE Trans. Geosci. Remote Sens.*, *44*(5), 1367–1379, doi:10.1109/TGRS.2006.873233.

Read, W. G., et al. (2007), Aura Microwave Limb Sounder upper tropospheric and lower stratospheric $H_2O$ and relative humidity with respect

to ice validation, *J. Geophys. Res.*, *112*, D24S35, doi:10.1029/2007JD008752.

Rodgers, C. D. (1976), Retrieval of atmospheric temperature and composition from remote measurements of thermal radiation, *Rev. Geophys.*, *14*, 609–624, doi:10.1029/RG014i004p00609.

Rodgers, C. D., and B. J. Connor (2003), Intercomparison of remote sounding instruments, *J. Geophys. Res.*, *108*(D3), 4116, doi:10.1029/2002JD002299.

Russell, J., et al. (1993), The Halogen Occultation Experiment, *J. Geophys. Res.*, *98*, 10,777–10,798, doi:10.1029/93JD00799.

Schoeberl, M., et al. (2007), A trajectory-based estimate of the tropospheric ozone column using the residual method, *J. Geophys. Res.*, *112*, D24S49, doi:10.1029/2007JD008773.

Schoeberl, M. R., et al. (2006a), Overview of the EOS Aura mission experiment, *IEEE Trans. Geosci. Remote Sens.*, *44*(5), 1066–1074, doi:10.1109/TGRS.2005.861950.

Schoeberl, M. R., et al. (2006b), Chemical observations of a polar vortex intrusion, *J. Geophys. Res.*, *111*, D20306, doi:10.1029/2006JD007134.

Schoeberl, M. R., et al. (2008), QBO and annual cycle variations in tropical lower stratosphere trace gases from HALOE and Aura MLS observations, *J. Geophys. Res.*, *113*, D05301, doi:10.1029/2007JD008678.

Schwartz, M. J., W. G. Read, and W. V. Snyder (2006), EOS MLS forward model polarized radiative transfer for Zeeman-split oxygen lines, *IEEE Trans. Geosci. Remote Sens.*, *44*, 1182–1191, doi:10.1109/TGRS.2005.862267.

Schwartz, M. J., et al. (2007), Validation of Aura Microwave Limb Sounder temperature and geopotential height measurements, *J. Geophys. Res.*, doi:10.1029/2007JD008783, in press.

Stajner, I., et al. (2008), Assimilated ozone from EOS-Aura: Evaluation of the tropopause region and tropospheric columns, *J. Geophys. Res.*, doi:10.1029/2007JD008863, in press.

Toon, G. C. (1991), The JPL MkIV interferometer, *Opt. Photonic News*, *2*, 19–21.

Walker, K. A., C. E. Randall, C. R. Trepte, C. D. Boone, and P. F. Bernath (2005), Initial validation comparisons for the Atmospheric Chemistry Experiment (ACE), *Geophys. Res. Lett.*, *32*, L16S04, doi:10.1029/2005GL022388.

Wang, H.-J., D. M. Cunnold, L. W. Thomason, J. M. Zawodny, and G. E. Bodeker (2002), Assessment of SAGE version 6.1 ozone data quality, *J. Geophys. Res.*, *107*(D23), 4691, doi:10.1029/2002JD002418.

Wang, H.-J., D. M. Cunnold, C. Trepte, L. W. Thomason, and J. M. Zawodny (2006), SAGE III solar ozone measurements: Initial results, *Geophys. Res. Lett.*, *33*, L03805, doi:10.1029/2005GL025099.

Wang, P.-H., et al. (2006), Ozone variability in the midlatitude upper troposphere and lower stratosphere diagnosed from a monthly SAGE II climatology relative to the tropopause, *J. Geophys. Res.*, *111*, D21304, doi:10.1029/2005JD006108.

Waters, J. W., et al. (2006), The Earth Observing System Microwave Limb Sounder (EOS MLS) on the Aura satellite, *IEEE Trans. Geosci. Remote Sens.*, *44*(5), 1075–1092, doi:10.1109/TGRS.2006.873771.

World Meteorological Organization (2003), Scientific assessment of ozone depletion: 2002, *Global Ozone Res. Monit. Proj. Rep. 47*, Geneva, Switzerland.

Wu, D. L., et al. (2008), Validation of the Aura MLS cloud ice content measurements, *J. Geophys. Res.*, doi:10.1029/2007JD008931, in press.

Yang, E.-S., D. M. Cunnold, R. J. Salawitch, M. P. McCormick, J. M. Russell III, J. M. Zawodny, S. Oltmans, and M. J. Newchurch (2006), Attribution of recovery in lower-stratospheric ozone, *J. Geophys. Res.*, *111*, D17309, doi:10.1029/2005JD006371.

Yang, Q., D. M. Cunnold, H.-J. Wang, L. Froidevaux, H. Claude, J. Merrill, M. Newchurch, and S. J. Oltmans (2007), Midlatitude tropospheric ozone columns derived from the Aura Ozone Monitoring Instrument and Microwave Limb Sounder measurements, *J. Geophys. Res.*, *112*, D20305, doi:10.1029/2007JD008528.

Ziemke, J. R., S. Chandra, B. N. Duncan, L. Froidevaux, P. K. Bhartia, P. F. Levelt, and J. W. Waters (2006), Tropospheric ozone determined from Aura OMI and MLS: Evaluation of measurements and comparison with the Global Modeling Initiative's Chemical Transport Model, *J. Geophys. Res.*, *111*, D19303, doi:10.1029/2006JD007089.

M. A. Avery, E. V. Browell, and J. W. Hair, NASA Langley Research Center, Hampton, VA 23681, USA.

P. F. Bernath, University of York, York YO10 5DD, UK.

C. D. Boone and K. A. Walker, University of Waterloo, 200 University Avenue West Waterloo, ON, Canada N2L 3G1.

R. E. Cofield, D. T. Cuddy, W. H. Daffer, B. J. Drouin, L. Froidevaux, R. A. Fuller, R. F. Jarnot, Y. B. Jiang, B. W. Knosp, A. Lambert, N. J. Livesey, G. L. Manney, J. J. Margitan, V. S. Perun, W. G. Read, M. J. Schwartz, B. Sen, W. V. Snyder, R. A. Stachnik, P. C. Stek, R. P. Thurstans, G. C. Toon, P. A. Wagner, and J. W. Waters, Jet Propulsion Laboratory, California Institute of Technology, 4800 Oak Grove Drive, Pasadena, CA 91109, USA. (lucien.froidevaux@jpl.nasa.gov)

M. J. Filipiak and R. S. Harwood, University of Edinburgh, Old College, South Bridge, Edinburgh EH8 9YL, UK.

K. W. Jucks, Harvard-Smithsonian Center for Astrophysics, 60 Garden Street, Cambridge, MA 02138, USA.

T. J. McGee, NASA Goddard Space Flight Center, Mail Code 130, Greenbelt, MD 20771, USA.

G. K. Sumnicht and L. W. Twigg, Science Systems Applications, Inc., 10210 Greenbelt Road, Suite 600, Lanham, MD 20706, USA.